BIOMEDICAL ENGINEERING MSc PROGRAM
UNIVERSITY OF CRETE
TECHNICAL UNIVERSITY OF CRETE
FOUNDATION FOR RESEARCH AND TECHNOLOGY-HELLAS

Biology of Stress
& Aging Lab

Application Grade Thesis

The TuReLi TTX assay plate:

Development of a Tunable and Reversible Linear Thermal Gradient Plate based on open-source modules for C. elegans thermotaxis assays

Spinthaki Sofia

Supervisor
Bazopoulou Daphne

Co-supervisor
Pantazis Alexandros

Heraklion 2023

This dissertation is submitted as a partial fulfilment of the requirements for the Master's degree of Biomedical Engineering M.Sc. Program

BIOMEDICAL ENGINEERING MSc PROGRAM
UNIVERSITY OF CRETE
TECHNICAL UNIVERSITY OF CRETE
FOUNDATION FOR RESEARCH AND TECHNOLOGY-HELLAS

Εργαστήριο Βιολογίας
Στρες & Γήρανσης

Μεταπτυχιακή Εργασία Επιπέδου Εφαρμογών

TuReLi TTX assay plate:

Ανάπτυξη συσκευής ρυθμιζόμενης και αντιστρεπτής γραμμικής μεταβολής θερμοκρασίας, ανοιχτού λογισμικού, για μελέτες θερμόταξης σε C. elegans

Σπινθάκη Σοφία

Επιβλέπουσα
Μπαζοπούλου Δάφνη

Επιβλέπων
Πανταζής Αλέξανδρος

Ηράκλειο 2023

Acknowledgments

I would like to thank the people without whom this work would not have been. My supervisors Dr. Bazopoulou and Dr. Pandazis for the opportunity, guidance and trust, the Biology of Stress and Aging Lab team for the great help on the biological protocol, George Makris and Dr. Deligeorgis for the crucial advice and discussion on technical design matters. Finally and always, thank you to Dr. Argyro Spinthaki.

Abstract

Thermal gradient platforms are used in a range of response testing applications from materials and components characterization i.e., glass transmission T ^{o}C, melting point, MFFT, to biology research. Thermotaxis (TTX) is the organism's locomotion strategy in response to environmental temperature changes or stimuli. This behavior ensures that organisms will locate themselves at optimal conditions and is the subject of nervous system studies. In the popular model organism *Caenorhabditis elegans*, TTX assays are employed for learning and memory studies i.e., how environmental signals shape behavioral output, with regards to previous experiences. During those assays, *C. elegans* navigate towards preferable isothermals when traveling up and down a thermal gradient. TTX assays require technical components that provide sensitivity, stability, high-resolution and/or high throughput capabilities. Commercially available equipment exists and requires minimum user expertise. However, this type of equipment drastically increases the cost while limiting potential output, since it is usually not compatible with other lab equipment. For that reason, research labs are turning into customized platforms that are tailored to their in house setup but have no provision for implementation from other users. Here, we developed a stand-alone, tunable TTX device: the TuReLi (Tunable, Reversible and Linear) TTX assay plate, from 3D printed parts and readily available modules, which allows high resolution multi-position temperature control and recording. Our system is open source-based, affordable to fabricate and requires no industrial control units. Due to the flexible and user-friendly operation, the TuReLi TTX is an ideal, universal solution for thermotaxis-based assays.

Περίληψη

Οι πλατφόρμες θερμικής βαθμίδας χρησιμοποιούνται σε εύρος εφαρμογών δοκιμής απόκρισης, από χαρακτηρισμό υλικών και στοιχείων π χ. θερμοκρασία υαλώδους μετάπτωσης, σημείο τήξης, ελάχιστη θερμοκρασία σχηματισμού φιλμ, ως βιολογικές μελέτες. Η θερμόταξη (TTX) είναι η στρατηγική μετακίνησης ενός οργανισμού, σαν απόκριση σε ερεθίσματα/αλλαγές θερμοκρασίας περιβάλλοντος. Αυτή η συμπεριφορά εξασφαλίζει ότι ο οργανισμός θα τοποθετηθεί σε βέλτιστες συνθήκες και είναι το αντικείμενο για μελέτες του νευρικού συστήματος. Στον δημοφιλή μοντέλο οργανισμό *Caenorhabditis elegans*, οι αναλύσεις θερμόταξης χρησιμοποιούνται για μελέτες μάθησης και μνήμης: πώς τα περιβαλλοντικά σήματα στα οποία εκτίθεται ο οργανισμός επηρεάζουν τη συμπεριφορά, σε σχέση με την προηγούμενη εμπειρία του. Σε αυτές τις αναλύσεις, ο *C. elegans* κινείται προς προτιμητέες ισόθερμες διαδρομές ταξιδεύοντας είτε προς αύξουσα είτε προς φθίνουσα θερμοκρασία, στη θερμική βαθμίδα. Οι μελέτες θερμόταξης απαιτούν εξοπλισμό που να προσφέρει ευαισθησία, σταθερότητα, δυνατότητα εξαγωγής δεδομένων υψηλής ευκρίνειας ή/και ψηλού ρυθμού. Εμπορικός εξοπλισμός είναι διαθέσιμος με ελάχιστες απαιτήσεις εξειδίκευσης του χρήστη. Ωστόσο, τέτοιου τύπου εξοπλισμός έχει αυξημένο κόστος, ενώ συχνά είναι και μη συμβατός με άλλο εργαστηριακό εξοπλισμό. Γι' αυτό το λόγο, τα ερευνητικά εργαστήρια στρέφονται προς ιδιοκατασκευασμένες πλατφόρμες, προσαρμοσμένες να ταιριάξουν στο εκάστοτε setup, χωρίς όμως να υπάρχει πρόβλεψη για χρήση από άλλα εργαστήρια. Εδώ, αναπτύσσουμε μία αυτόνομη, ρυθμιζόμενη συσκευή θερμόταξης: το TuReLi (Tunable, Reversible and Linear) TTX assay plate, από 3D εκτυπωμένα και άμεσα διαθέσιμα εξαρτήματα, που επιτρέπει έλεγχο και καταγραφή θερμοκρασίας πολλαπλών θέσεων για υψηλής ευκρίνειας μελέτες. Το σύστημά μας είναι ανοιχτού λογισμικού, προσιτό στην κατασκευή χωρίς να απαιτεί εξωτερικές μονάδες ελέγχου θερμοκρασίας. Με ευέλικτη και φιλική προς το χρήστη λειτουργία, το TuReLi TTX είναι μια πλήρης λύση για μελέτες θερμόταξης.

Table of Contents

Lists

List of Figures

List of Tables

A. Introduction

A.1.Premise

Thermal gradient platforms are employed in standardized industrial or in lab-specific, prototype solutions. They constitute essential equipment in material sciences for defining properties of dispersion materials, synthetic resins, adhesives or for performing tests in coatings and paints. In biological sciences, thermal gradient platforms are used for evaluation of temperature effects and thermo-regulation in biological samples [1][2][3]. This work is a progress report on a thermal gradient prototype – the TuReLi TTX device –designed as a flexible, compact and affordable solution for thermotaxis assays, based on open-source modules and 3D printed components. Here, we used it to perform TTX on *C. elegans*, a model organism and an ideal biological system for basic research and translation studies that involve drug screening and disease modeling.

The introductory chapter consists of a two-part literature overview: one part for *C. elegans* and one for existing thermotaxis devices. In the second chapter, we describe the prototype, including components, operation and notes of attention. In the third chapter, we report *C. elegans* methodologies and experimental results. In the last chapter we discuss the experimental outcomes and suggest future add-ons.

A.2.Literature – *C. elegans*

C. elegans is a microscopic non-parasitic self-fertilizing soil nematode that feeds on bacteria, specifically *E. coli* when cultivated in the lab. They grow at rates that depend on the environmental temperature which should ideally vary between 15-25 ^{o}C [4]. At 20 ^{o}C, laid *C. elegans* eggs will grow into Day 1 adults going through L1 to L4 larva stages in ~60 hrs. Day 1 adults will live an average of 3 weeks depending on temperature and genetic background. Their short generation time, ease of cultivation/inbreeding along with their transparent body and fully annotated genome with 80% similarity to human genome [5][6][7], make *C. elegans* a popular model organism for understanding fundamental biological and disease mechanisms. *C. elegans* became the first multicellular organism

with a mapped nervous system [8][9], composed of only 302 neurons. This advancement along with its amenability to genetic modification, allowed the dissection of molecular events that govern neurodevelopment, neuronal function and facilitated studies of neural circuits.

Figure 1. The nematode *C. elegans* [10]

During navigation, *C. elegans* perceive and process with high accuracy sensory inputs such as humidity, chemicals, light, temperature, electrical signals that affect their physiology or indicate the existence/absence of food/enemy etc. They evaluate their surroundings and adjust their navigation tactics, locomotion gait/sequences of movement to migrate to preferred more viable environments [6] [11]. *C. elegans* also exhibits experience-dependent plasticity in the form of learning and memory [4]. Studying how these animals process sensory signals can help unravel connections between behavior regulation and neural activity at a circuit or single neuronal level. Typical experimental strategies and methods used include genetic-based or laser ablation of neurons, calcium sensors as indicators of neural activity, light-gated ion channel to control neuronal excitability and quantitative behavioral tracking that characterizes locomotion patterns [12][13].

C. elegans can perform thermotaxis, a directed movement toward thermally optimal regions, that helps them regulate their body physiology and metabolism. When worms are placed on a temperature gradient, they can navigate towards the previous cultivation temperature [12][14]. For example, young (Day 1), wild type adult worms migrate to temperatures around or lower than 23 ^{o}C, if these temperatures were previously associated with the presence of food. Older animals (Day 6) show cryophilia after exposure to cultivation temperatures of < 22 ^{o}C. Starved animals of all ages exhibit athermotactic behavior [9][15][16]. Measuring thermotaxis behavior as a function of encoded temperature memory is a challenging task due to *C. elegans*' increased temperature sensitivity.

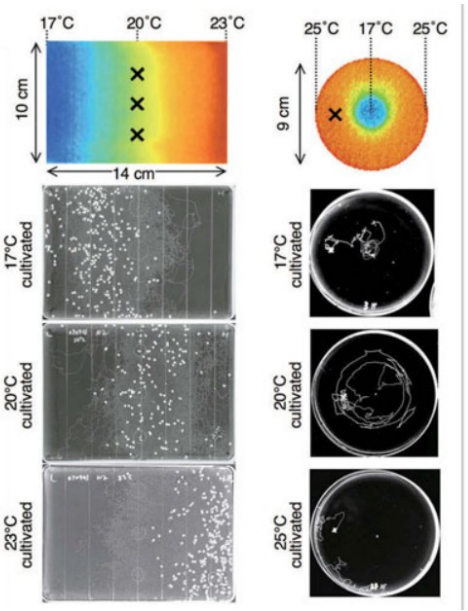

Figure 2. Example of linear and radial thermotaxis assay population imaging and worm tracking [14]

C. elegans has shown an isotherm tracking deviation of 0.05 °C within 3 °C of their cultivation temperature [17] or 0.01 C/cm, according to Luo et al., 2006 [6]. Gradients steeper than 0.5 ºC/cm and greater distances from the cultivation temperature than 5 ºC may disrupt the thermotactic behavior [1] [12][13]. A suggested interpretation is that animals rarely encounter abrupt temperature changes in nature [18].

Thermotaxis assays require the generation of a stable and precise temperature gradient which is tightly controlled and constantly monitored. The temperature range is usually set at either between 18-31.5 °C or 23-36.5 °C [19] in linear or radial gradients. Duration of assays varies from 45 minutes up to two hours [11]. Factors that can negatively affect worm performance during the assay [4] are population density, humidity on assay plate, prolonged stay of *C. elegans* in liquid buffers, unwanted odors and dry/cracked medium in plates.

A.3.Literature – state of the art

From industrial to research applications, there is a variety in thermal gradient surface devices. Commercially available devices like the CPV thermal gradient bar (TECA. FEATURES) [2], the

GRD1 temperature gradient plate from Grant Instruments (Cambridge) Ltd [3] or the one from Industrial Physics, LLC [1], tend to be more robust in their performance. They weigh up to 300 kg, have a temperature set range from −30 ºC to +250 °C and can perform in simultaneous assays. They feature a standard deviation of 0.5± ºC and a setting temperature resolution of 1.0 ºC. Equipment used for the gradient formation include cold plates (e.g., LHP-800CP from Teca Corp., Chicago), hot plates (e.g., Corning model PC320), water blocks (eg. from Swiftech) and bath recirculators (e.g., AC150 from Thermo Fisher Scientific & VWR) with liquid pumps (e.g., from Tokai Hit) or peltiers/thermoelectric coolers (TEC) (e.g., from Ferrotec) [11].

Custom made lab devices do not require high expertise and can have adequate operation compared to standard industrial solutions [18]. Peltier modules (TECs) are in this case the preferred thermoelectric components for gradient formation. They are low cost, small and light and can have both cooling and warming uses. TECs can directly create temperature difference at the junction of two different types of materials when electric current passes through[20]. The Peltier effect is described by the equations:

$$P = Q/I \quad (1)$$

where I – current, P - Peltier coefficient.

$$\Delta T = (V_{OC}/(Th - Tc)\, T_c\, I - 0.5\, I^2\, R - Q_c)/K \quad (2)$$

where Qc - cooling capacity, V_{OC} - open circuit voltage, Tc - cold side temperature, T_h - hot side temperature, R - resistance, K - thermal conductivity. Peltiers for gradient formation have been used in a low-throughput microfluidic system for *C. elegans* thermotaxis analysis that was developed using PDMA & soft lithography [7].

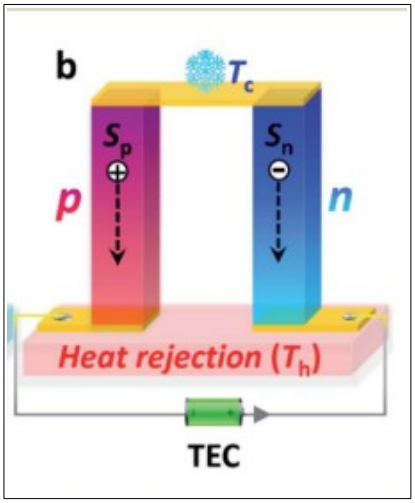

Figure 3. Thermoelectric component, single-unit operation [20]

The gradient is formed on aluminum slabs placed on top of the heating or cooling units. Alternatively, glass plates may be used coated with heat conductive indium tin oxide (ITO) [5]. For temperature monitoring, thermocouples and 3-wire platinum resistance temperature detectors Pt-RTDs are used as sensors [13]. The reservoir temperature is maintained with a H-bridge amplifier (Newport Electronics) and one or two conventional industrial PID controllers like SDU440 (from Sanup Electric) [11] or HTC3000 (from Wavelength Electronics) [17]. H-Bridges are circuits used to control speed and direction of DC motors. In a simplistic representation, the circuit consists of four switching elements – an arrangement of transistors, that switch the polarity of a voltage applied to a load. The name is derived from its schematic, as shown in the image below.

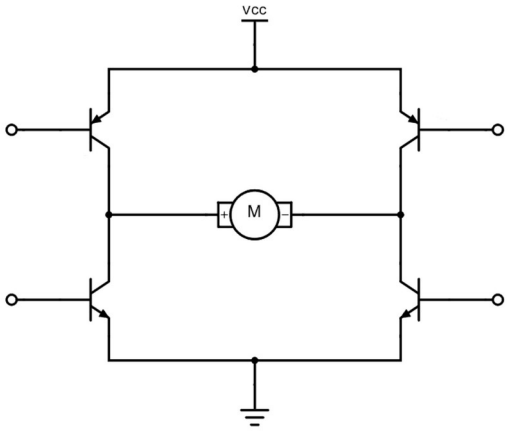

Figure 4. Schematic diagram of an H-bridge circuit

H-Bridges are used with a microcontroller, such as an Arduino. The Arduino controls the H-Bridge with Pulse Width Modulation and PID through two separate input pin-sets for each output. PID stands for Proportional Integral Derivative and is used on devices to ensure the best possible stability when maintaining a measured value at a desired setpoint. For the calculation of the output, the following equation is used:

$$u(t) = K_p\, e(t) + K_i \int e(t)dt + K_p\, de/dt \qquad (3)$$

where u(t) - PID control variable, K_p - proportional gain, e(t) - error value, K_i - integral gain, de - change in error value, dt - change in time. K_P drives the control variable in proportion to the instantaneous error, K_I drives it in proportion to the accumulated error, and K_D drives it in proportion to the instantaneous rate of change of the error. When designing a system, the K_P, K_I, K_D parameters are tuned to adjust the reaction of the controllers to set-point changes and disturbances [21]. Advantages of this type of control include the quicker response time due to the P-only control and decreased offset due to the combined D and I control.

B. The Prototype

B.1. The Prototype – Design & Construction

The objective was to follow a simplistic manufacturing approach while maintaining adaptability on operating settings and ease of use. We aimed at a compact and lightweight design, simple to operate and/or repair with each part easily removable and replaceable. We also aimed to use low cost parts, readily available in hardware stores and retail metal suppliers. The prototype consists of three modules: the frame, the control unit and the plate (Appendix B).

B.1.i. Frame

The parts of Table 1 were used for assembling the frame. Parts 1-5 were purchased from a metal supplier. Parts 6-10 are 3D printed with PLA filament. For the 3D printing process, the parts where designed on Fusion 360 from Autodesk, the models were sliced using PrusaSlicer2.4.2 and the printer used was the Prusa i3 MK3S.

The parts of the frame are included in the following table:

Table 1: The frame – components

Part number	Part quantity	Part	Part acquisition
1	4	20 cm, diameter ⌀ 6 mm rod	metal supplier
3	4	12 cm, diameter ⌀ 6 mm rod	metal supplier
4	2	10 cm, diameter ⌀ 6 mm rod	metal supplier
5	14	Diameter ⌀ 0,6 mm screws	hardware store
6a	1	PCB base	3DP
6b	4	box base	3DP
7	2	fan support	3DP

8	4	lower joint	3DP
9	4	upper joint	3DP
10	1	H-bridge extension	3DP

Part 6a: PCB base is designed as an enclosure bottom to fit the device electronics (Image 5a).

Part 6b: Box base prints are holders that adjust to the lower rods, and parts like 6a can be screwed on them (Image 5b).

Part 7: Fan support includes brackets that fit in the fans (Image 5c).

Part 8: Lower joint can hold three ⌀6mm rods and is used to screw the whole device to an optical breadboard (Image 5d).

Part 9: Upper joint can hold two ⌀6mm rods, each stabilized with a screw, so that each distance of the frame can be adjusted separately (Image 5e).

Part 10: H-bridge extension. The H-bridge board used requires cooling so it is mounted outside of the PCB box (Image 5f). This part is mounted on part 6a.

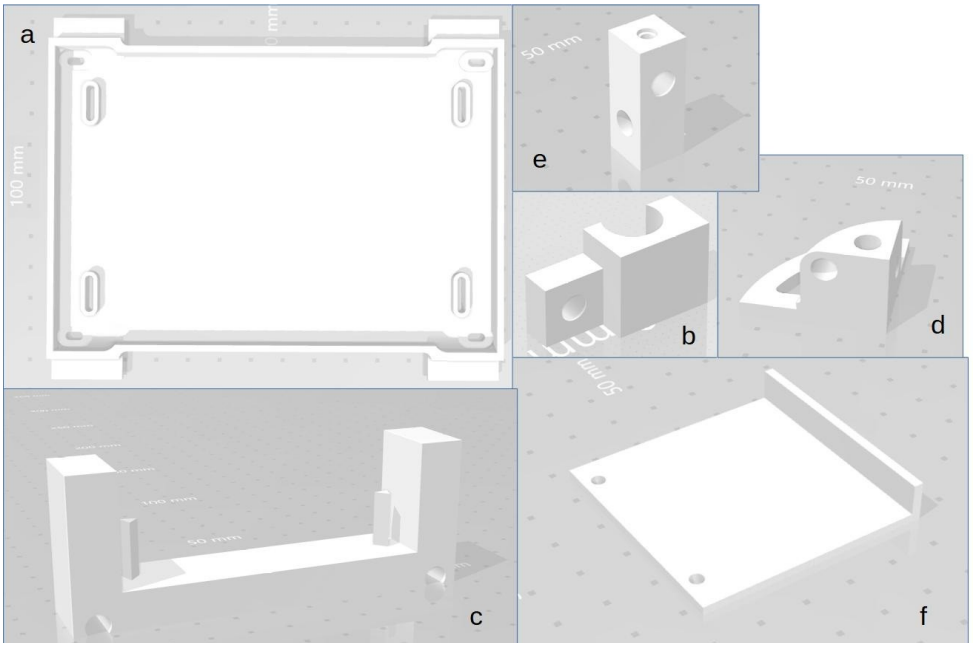

Figure 5. Building blocks of the frame (not in scale, Table 1). a: part 6a, PCB base model; b: part 6b, box base model; c: part 7, fan support model; d: part 8, lower joint model; e: part 9, upper joint model; f: part 10, H-bridge extension model.

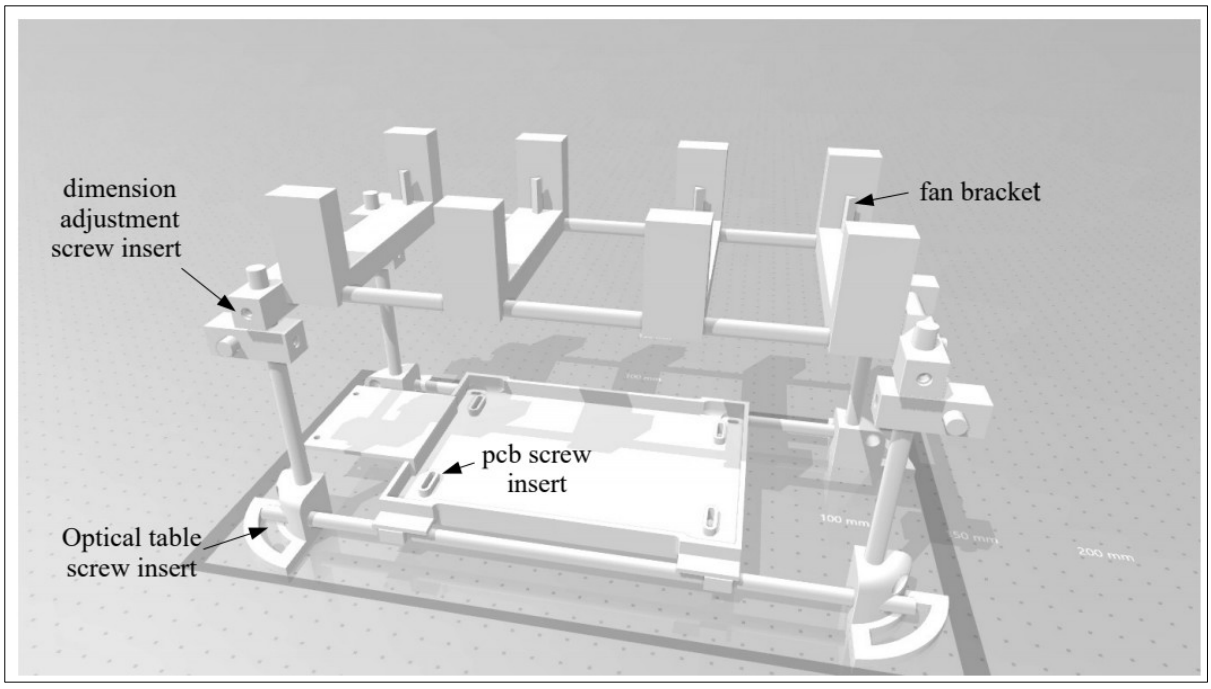

Figure 6. The frame

The distance of the fan holders and hence the edges of the temperature gradient can be modified either before or during an assay. The measurement area can be from 0 to 8 cm, allowing the use of different plates. All parts of the frame are estimated to cost ~7€.

B.1.ii. Control unit

In this part, we describe the circuit board construction procedure and the assembling of the electronic components of the device.

The circuit was designed using KiCad software.

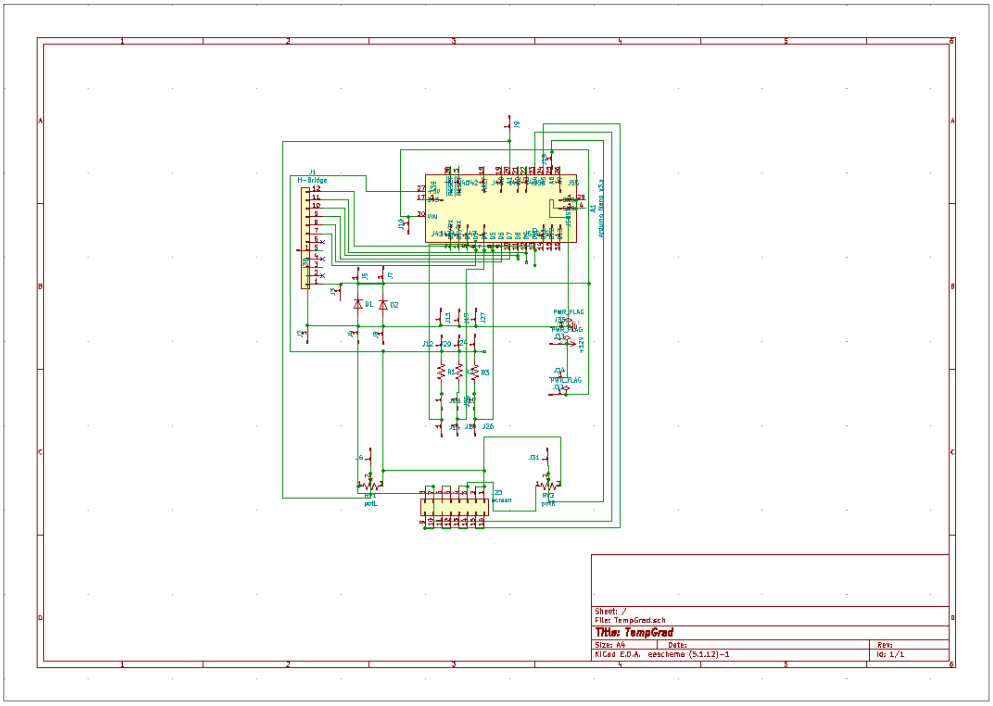

Figure 7. PCB schematic

The schematic was printed as a board mask on two transparencies (to achieve higher opacity of mask).

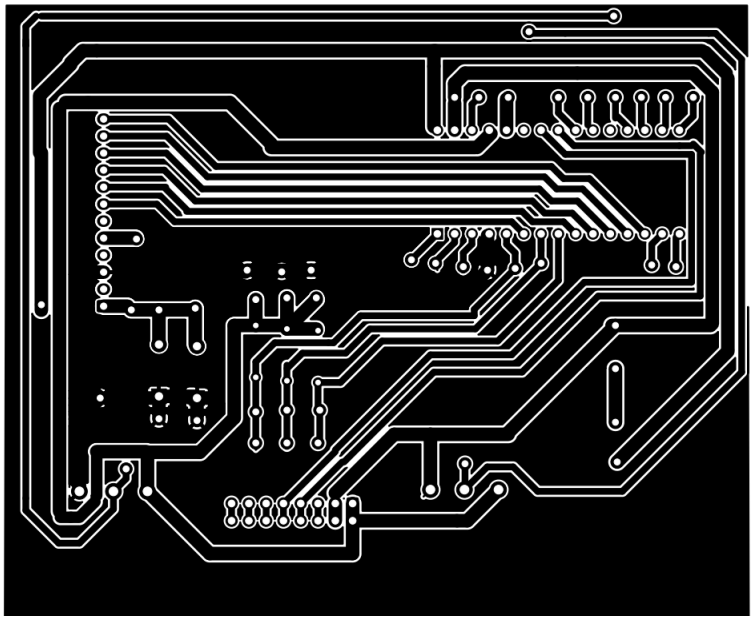

Figure 8. PCB mask

The transparencies were placed on a positive photosensitive copper board which was then exposed to sun light for 2 minutes. The board was immersed in a potassium hydroxide solution for 1½ minutes to remove the exposed photosensitive material. Then it was immersed in a ferric chloride solution for ~20 minutes, regularly stirred, for de-coppering. Duration of all steps depends highly on solution concentration (and sunshine, for the first step). After proper cleaning, tinning and drilling, the board is ready to be soldered. The components are found in Table 2. Components 3, 4, 5 and 8 were plugged on pins, not directly soldered on the board.

Table 2: Control Unit – components

Component number	Component quantity	Component
1	3	4.7kΩ resistor
2	2	1N4001 diode
3	1	Arduino Nano Atmega328
4	1	SSD1306 OLED display

5	2	L298N H-bridge module
6	2	2-Wire fan
7	2	TEC1-12704 peltier module
8	2	100k linear pontesiometer
9	3	DS18B20 thermometer module
10	1	switch
11	1	12V plug
12	2	Heat sink

Component 1: Resistors are used for the wiring of the temperature sensors. Each resistor is connected to the positive and data wire of each of the three sensors.

Component 2: Two diodes are wired across each fan to eliminate voltage spikes from a sudden supply current reduction/interruption (flyback).

Component 3: The Arduino Nano is an open hardware development microcontroller board which is used here to set the temperature at the edges of the gradient plate.

Component 4: The screen displays the set left temperature (value of the cor/ing ‘left’ potensiometer), the real left temperature (value of the cor/ing ‘left’ Dallas sensor), the set right temperature (value of the cor/ing ‘right’ potensiometer), the real right temperature (value of the cor/ing ‘right’ Dallas sensor) and the indication of the third temperature sensor during the assay.

Component 5: L298N H-bridge motor control modules are used here for the peltier modules control, by controlling the voltage value and polarity at two separate outputs for the two peltiers. Two H-Bridge modules are connected in parallel for better I(A) supply to the TECs.

Component 5: The bridge motor control modules control the voltage value and polarity at two separate outputs for the two peltiers. They are connected in parallel for better I supply to the TECs.

Component 6: The 80×80×25 mm fans are used for the cooling of the TECs.

Component 7: The TEDs have a range in working temperature from -55 ^{o}C to +80 ^{o}C.

Component 8: The user manually sets the temperature before or during an assay on the left and right side of the gradient plate by adjusting the corresponding potensiometer.

Component 9: Thermometers have a range from -55 ºC to 125 ºC and ±0.5 ºC accuracy. Two of the thermometers are used in the PID control feedback loop and one for an extra measurement, either of the room temperature, or of a selected location on the plate.

Component 10: On-off switch of the H-Bridge, peltier modules and fans.

Component 11: Power input for the H-Bridge, peltier modules fans and the micro-controller when the device is not connected to a computer.

Component 12: 70×97×25 mm aluminum heat sinks for the cooling of the TECs.

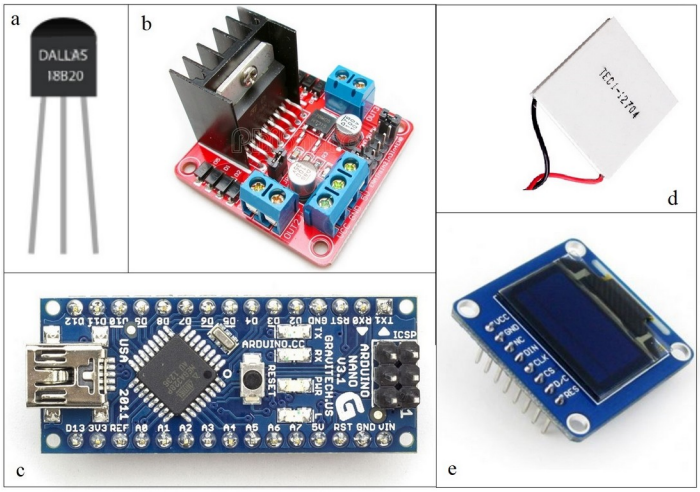

Figure 9. The basic modules from Table 2. a: part 9, DS18B20 temperature sensor; b: part 5, L298N H-bridge; c: part 3, Arduino Nano Atmega328; d: part 7, TEC1-12704 peltier module; e: part 4, SSD1306 OLED display.

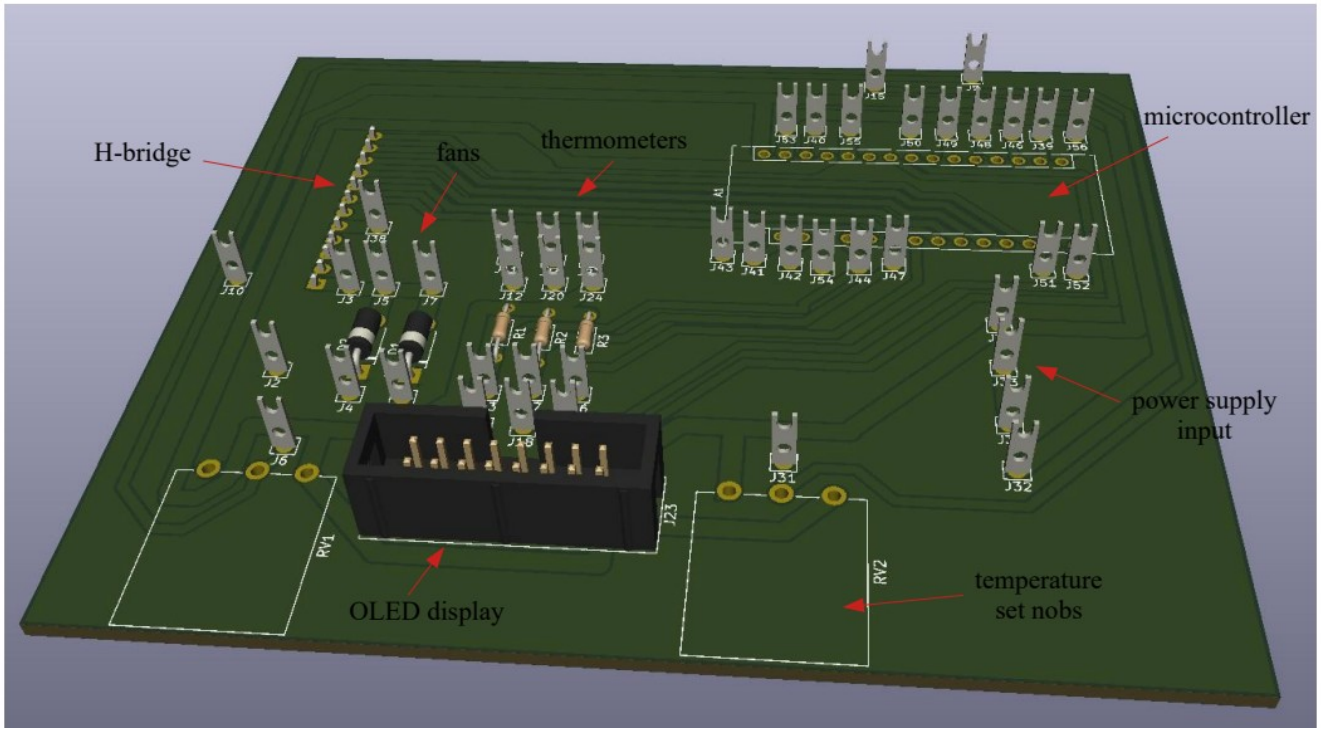

Figure 10. PCB model

For assembly, the PCB is bolted on the PCB Base, (Table 1, part 6a, frame), the H-bridge is bolted on the H-bridge extension (Table 1, part 10, frame) and the fans are adjusted on the fan support parts (Table 1, part 7, frame). The heat sinks are placed on top of each fan and the peltiers are stabilized on top of each heat sink with thermal paste (thermally conductive, electrically insulating compound). All parts of the control unit are estimated to cost 65-75€ cost.

For all modules, there are freely available sketches online or in the IDE Libraries. The complete sketch developed and uploaded on the Nano is included in Appendix A.

B.1.iii Plate

The plate consists of two parts (Table 3): the aluminum surface on which the gradient is formed and a 3D printed PLA (polylactic acid) plate. The two parts are glued together using thermally insulating silicon paste.

It is easy to create a thermal gradient on an aluminum surface, where the thermal conductivity is high. This is not the case with agar medium-plated petri dishes – the conventional maintenance environment for *C. elegans* populations, due to the thermally insulating plastic petri dish. To counteract this, previous studies have used either a glycerol layer between the plate and the dish or petri dishes with openings for aluminum parts to connect to directly to the agar. Both approaches were tested here but we eventually opted for the glycerol since this can be more easily implemented by other users as well. The parts of the plate are included in the following table:

Table 3: Gradient plate – components

Part number	Part quantity	Part	Part acquisition
1	1	Aluminum plate	metal supplier
2	1	Insulation plate	3DP

Part 1: Aluminum is chosen for its high thermal conductivity, low weight and low cost.

Part 2: This part serves as an insulator to minimize thermal losses from the bottom of the aluminum plate to the environment.

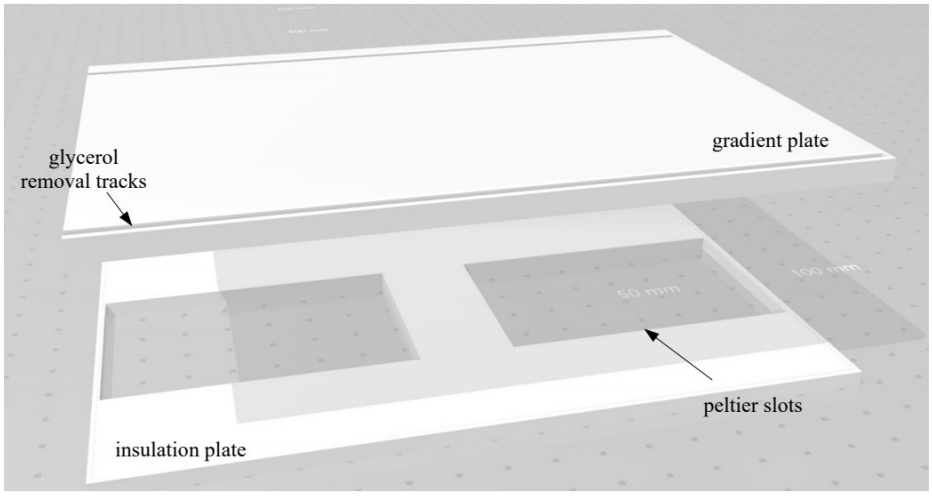

Figure 11. The thermal gradient plate

The plate is located on the top of the setup and the peltiers fit in the slots of the PLA plate and are in contact with the aluminum plate. Thermally conductive paste is applied between the aluminum bottom surface and the peltiers for better heat diffusion. The parts of the plate are estimated to cost ~3€.

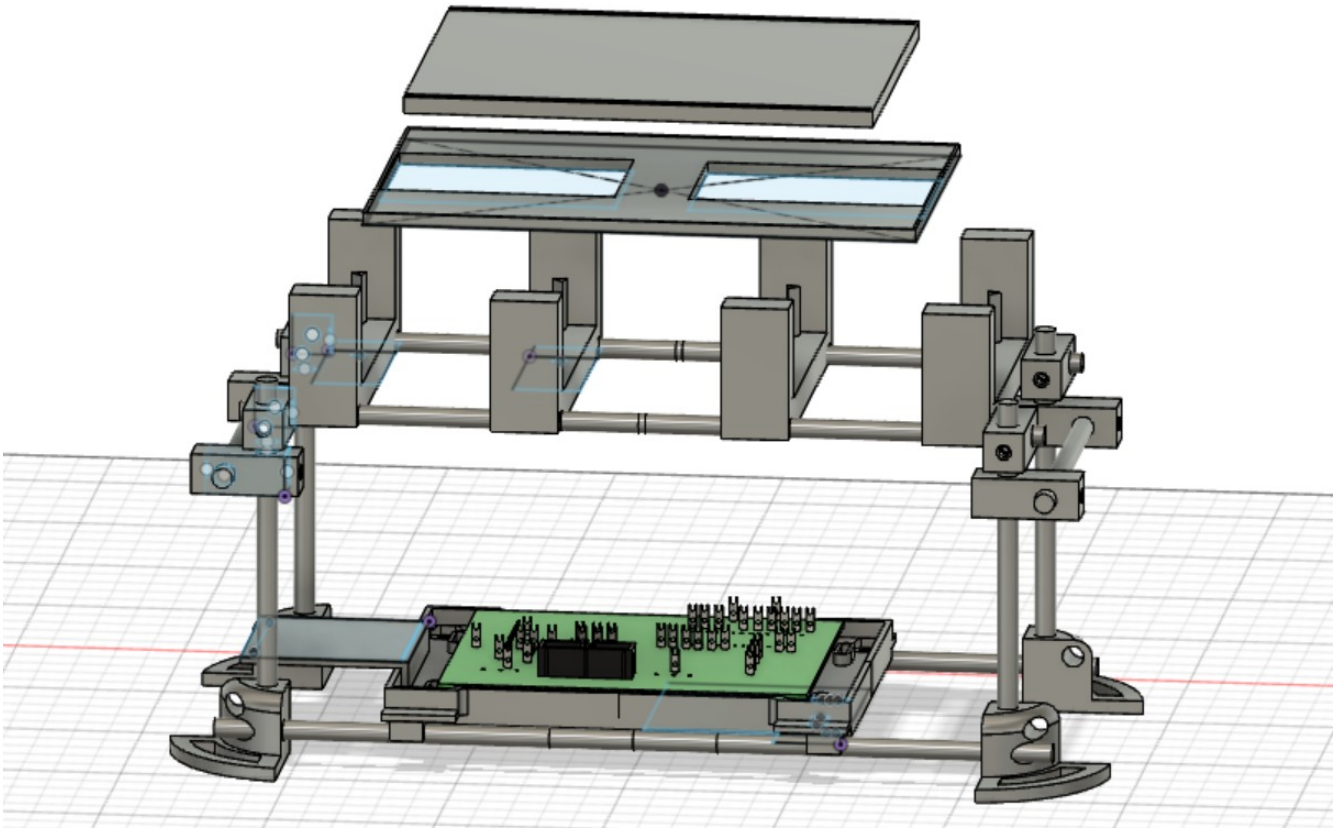

Figure 12. Schematic of the parts of device (view by Fusion 360º). The PCB, with connection pins for the temperature control modules, is shown bolted on the fully assembled frame.

B.2. The Prototype – Operation & Characterization

TECs have a working range from -30 to 70 ºC. However the device is set to operate from 5 to 45 ºC at both sides (see sketch), taking into account the lab room and *C. elegans* natural habitat temperature. The user, through the Arduino IDE environment may control the K_P, K_I and K_D parameters and the potentiometer settings to set the temperature range. However, these adjustments in the device tuning requires attention. For example, a large $\Delta T = |T_{real} - T_{set}|$ demands higher K_P but $\Delta T_{high} = |T_{room} - T_{set\_high}|$ and $\Delta T_{low} = |T_{room} - T_{set\_low}|$, where T_{set_low} and T_{set_high} are the user-defined gradient edge

temperatures, are not exclusively equal. This means that if the K_{P_high} and K_{P_low} are left to default, the time it takes for $\Delta T_{high} = 0$ and $\Delta T_{low} = 0$ will differ. In that case, it takes up to 1 extra minute for the gradient to reach a steady state, after both $\Delta T_{low} = \Delta T_{high} = 0$.

As mentioned earlier, any changes in the setup are to be followed by re-tuning of the K_P, K_I, K_D parameters in the sketch to optimize its performance, as it became clear during the construction of the device. In Figure 13 the system response is shown: the change of T_{real} with time until it reaches T_{set}. On 1b (left) only the low T side is operating and on 1b (right) is the full operation of the gradient but without re-tuning, where the high T side is under-performing (blue arrow).

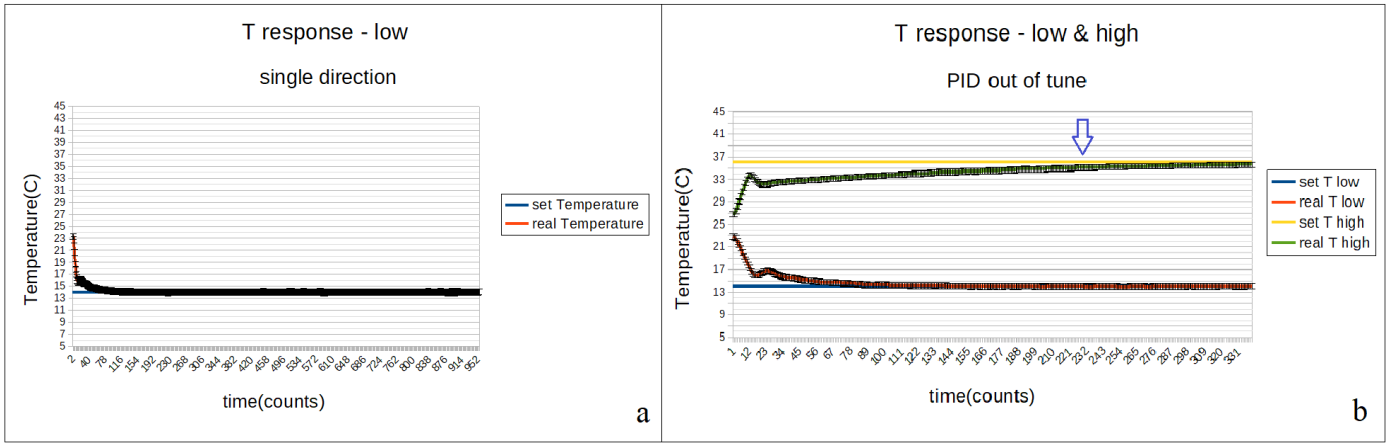

Figure 13. a: Single-temperature time response of the device. B: Full gradient time response before re-tuning

In Figures 14, 15, 16, we see the temperature response of the device in time, at different steps of the performance optimizing procedure. The goal is to achieve a relatively quick formation of an oscillation-free gradient in the agar of the dish. For this in the final step, the device is re-tuned after glycerol is added between the plate and the dish.

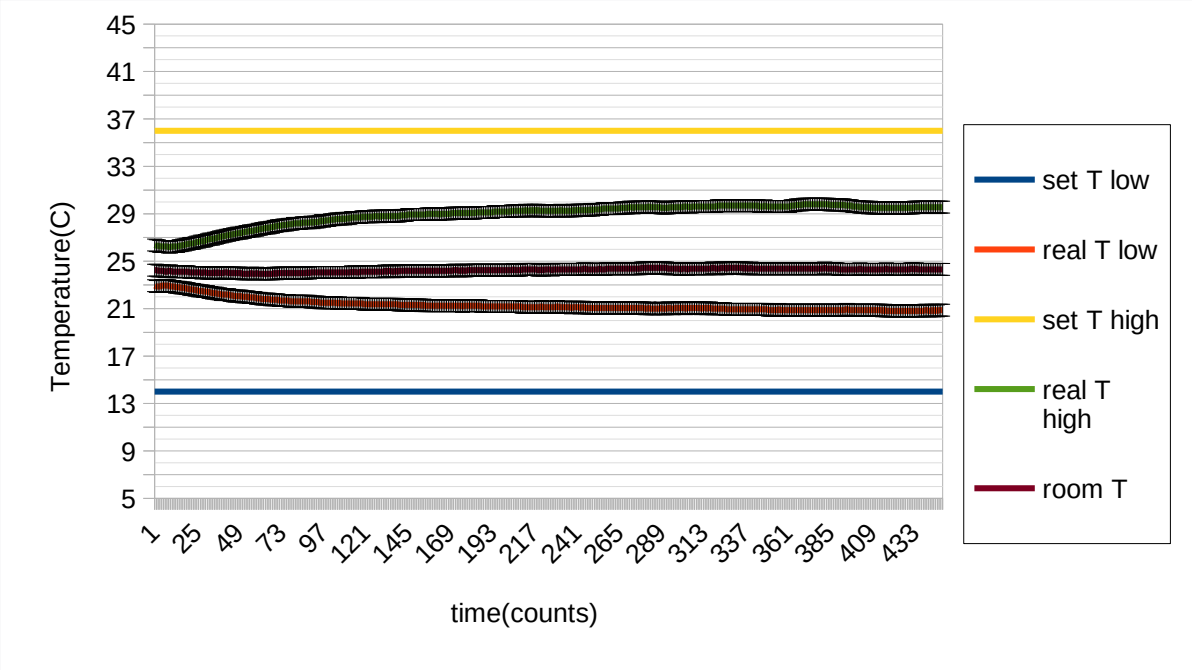

Figure 14. Gradient in the petri dish with no glycerol on the gradient plate

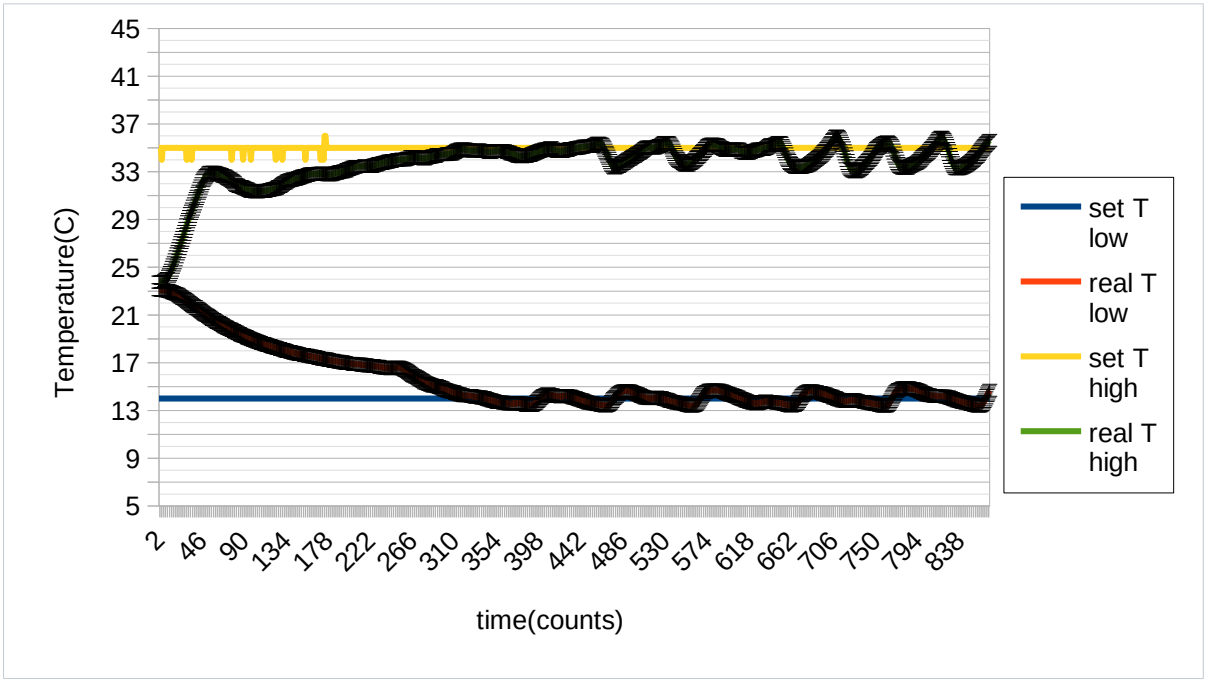

Figure 15. Gradient in the petri dish with glycerol on the gradient plate, before re-tuning

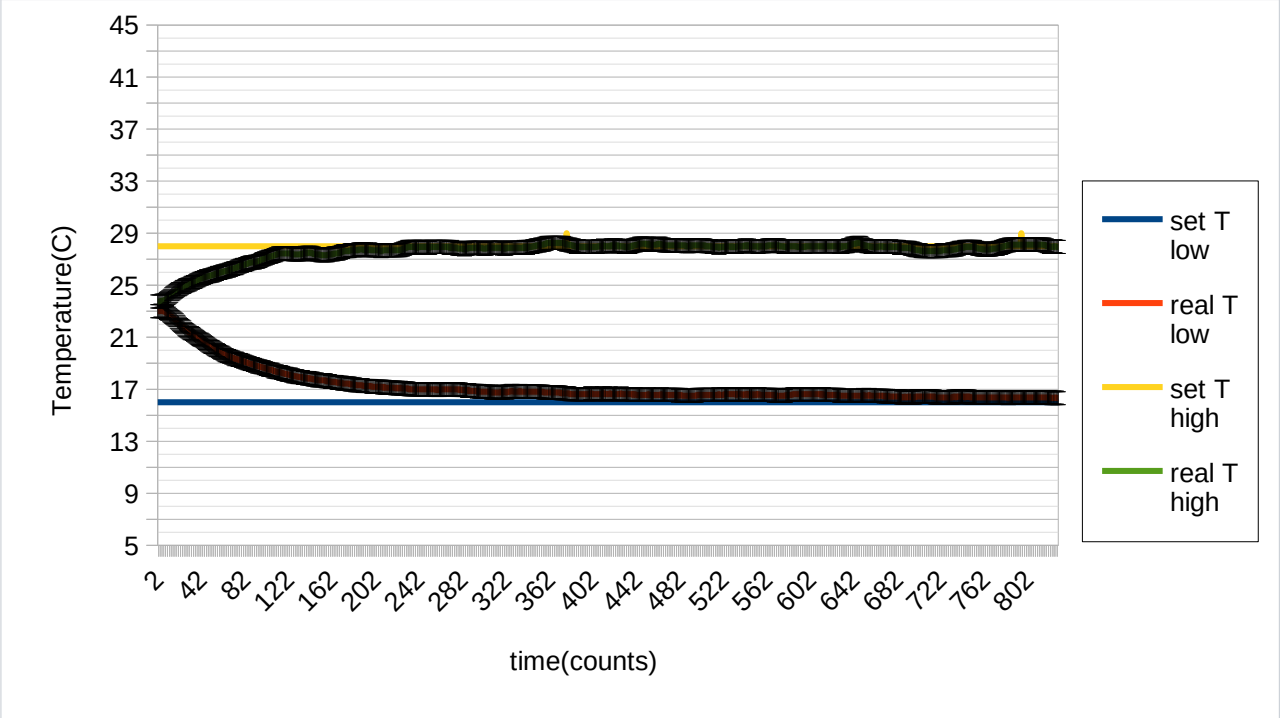

Figure 16. Gradient in the petri dish with glycerol on the gradient plate, after re-tuning

Each side reaches steady state in up to 5 minutes eg. t_s = 0 min if set T = T_{room} but t_s = 5 min if set T = 14 ºC. It takes up to ~7 minutes to reach full steady gradient state. During the assays, deviation was ±0.2 to ±0.4 °C, for 80 minutes test runtime, which is within the expected error rate of Dallas temperature sensor (~0.5 °C). In Figure 17, we see the temperature response at edges of the gradient in time, for et T_{low} = 15ºC and set T_{high} = 27 ºC.

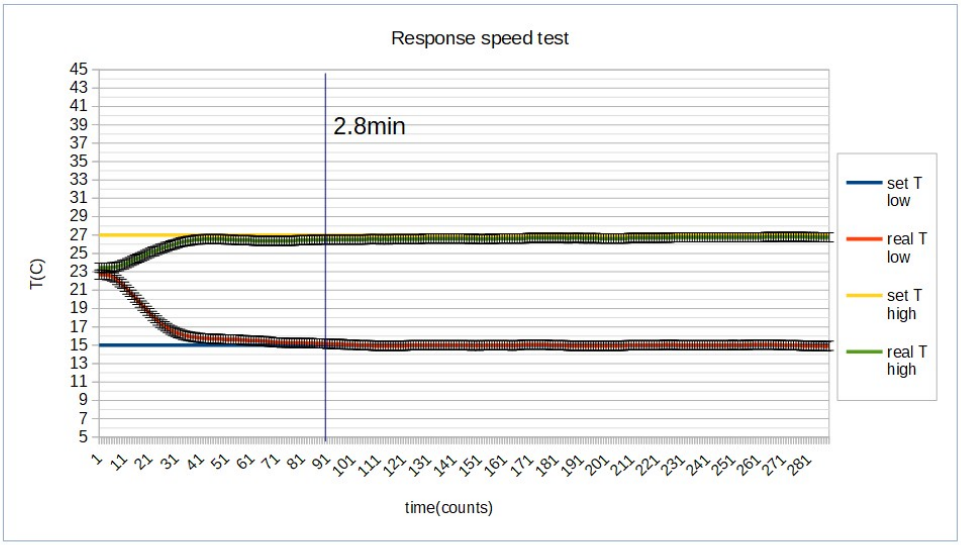

Figure 17. Response speed test for set T_{low} = 15 ºC and set T_{high} = 27 ºC, time to steady state 170 sec

For the gradient linearity monitoring and for clustering the worm location results during the assays, a 'grid-lid' is used. A (10×10) cm common petri dish lid that is marked with columns from A to J and rows from 1 to 10 forming a 1 cm unit grid and with openings for inserting the Dallas (Figure 18).

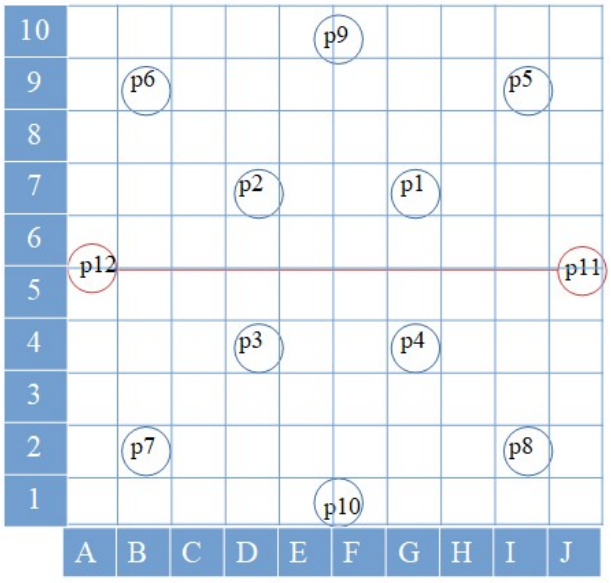

Figure 18. Petri grid lid representation with sensor positioning for temperature control

Positions (p#) 11 & 12 are for positioning feedback-loop control thermometers. During random assays, the thermometer 3 is placed on a different positions p1 through p10 for gradient linearity monitoring. To extract the response equations from the thermometer measurements, those positions are assigned distance coordinates (x,y), measured in half square. The y distance zero is set at the middle (red line) and the x distance zero is set at column A on the left of the dish. For example, the coordinates (x,y) of position 8 are p8(8,-3.5). The characterization equation:

$$T\,(C) = (1/9)*(T_{p11} - T_{p12}) * x\,(cm) + T\,(x_0),\ R^2 = 0.994 \qquad (4)$$

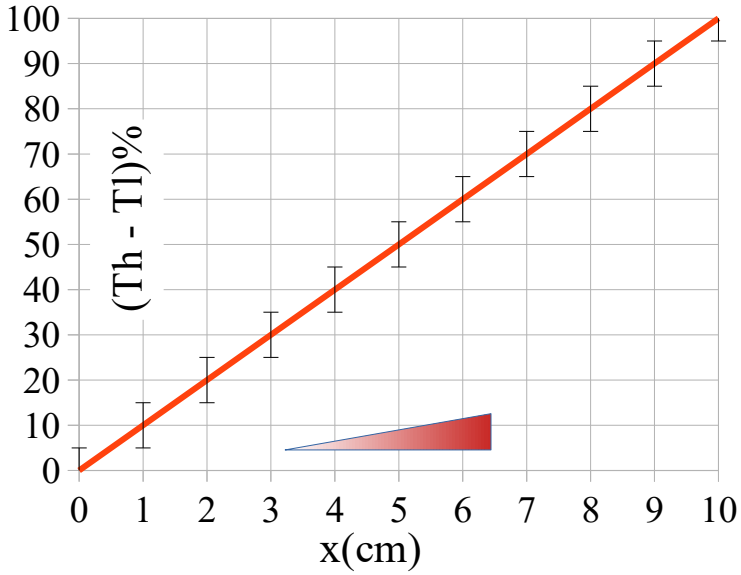

Figure 19. Gradient linearity in petri dish

R^2 is found from 0.985 to 0.999 and the R^2 spatial variation measured on these randomly selected assays is shown in Figure 20 below where values near the center of the x axis of the gradient are found to be closer to 1, regardless the y distance.

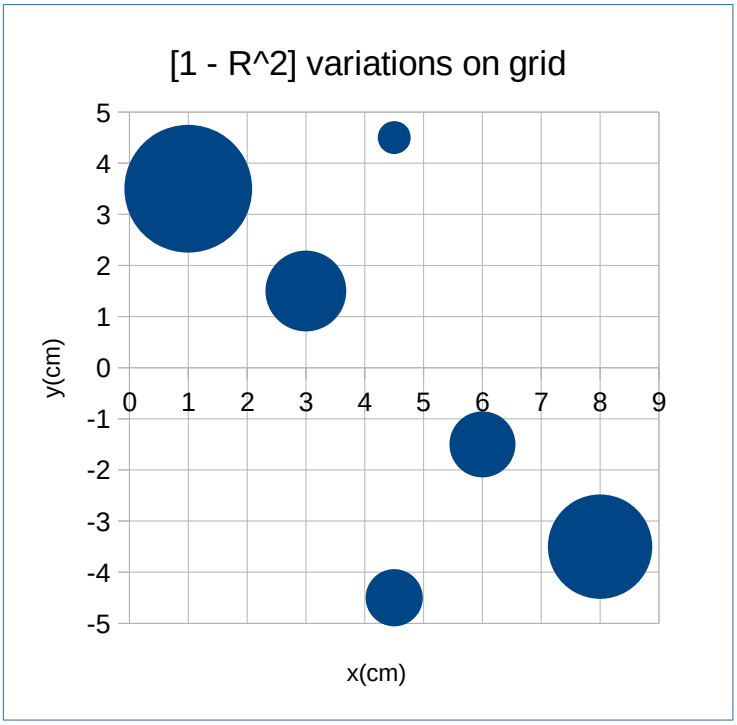

Figure 20. Spatial variation of linearity on grid: $0.985 \leq R^2 \leq 0.999$

Note1: From this point, all temperatures refer to values measured in the agar plate, which differ from the ones on the alouminium plate by at least 1.5 ºC. This does not include thermometer 3 measurements as it is used for T_{room} monitoring.

Note2: For temperature ranges with between 17-28 ºC, that match the needs of *C. elegans* thermotaxis trial assays (see Chapter C), we provide the Arduino code in Appendix A. For other temperature ranges, the used can adjust the K_P, K_I, K_D accordingly.

Instructions for use:

1. Plug in 12V3A power supply
2. Select PC-powered mode of the micro-controller for temperature recording or power supply-powered mode for device autonomy, by switching position of the on-board shortcut.

- In case of the PC-powered mode, connect the micro-controller to the USB and open Arduino IDE environment.
- Select the correct board and port
- Open the serial monitor

3. Confirm the thermometer measurements.
4. Prepare the assay dish (see chapter C. Thermotaxis Assays)
5. Put glycerol on the plate and then the dish on top. Ensure that the glycerol covers the dish bottom surface evenly.
6. Replace the lid of the plate with a grid-lid and place the two feedback loop thermometers in the holes/positions 11 and 12, so that the sensors are completely submerged into the agar.
7. Press the on-off button on the board to start the assay

C. Thermotaxis Assays

C.1. Thermotaxis Assays – Methodology of experiments

Before the assay:

Wild-type *C. elegans* strain are bred in the lab using standard techniques [22]. They are cultivated on 6 cm diameter petri-dish plates with agar-based nematode growth medium (NGM). *Escherichia coli* strain OP50 is seeded on the plate as bacterial food. Worms are cultivated from eggs to Day 1 (young) adults at 20 ^{o}C, for 72 hours. The assays plates are 100×00 mm squared petri dishes with NGM. NGM powder ingredients: 3 g/l NaCl, 2.5 g/l of BactoPeptone and 17 g/l BactoAgar. After autoclaving, the medium is allowed to cool and is supplemented with 1000 ml/l $CaCl_2$, 1000 ml/l $MgSO_4$, 25 mL of $KHPO_4$, 1000 ml/l cholesterol in ethanol solution, 1000 ml/l nystatin and 1000 ml/l streptomycin. M9 medium is used to wash off and collect worms from NGM plates. For M9, 3g/l KH_2PO_4, 6g/l Na_2HPO_4, 5g/l NaCl are diluted and stirred until dissolved to ddH_2O. After autoclaving, 1mL/l of 1 M $MgSO_4$ is added. The buffer is stored at room temperature for two weeks.

During the assay:

Uncrowded/well-fed Day 1 adult animals as well as mixed crowded populations maintained at 20 ^{o}C were used for the TTX trial assays. The animals were collected and washed with 5 ml of M9 basal buffer and placed on the dish, at different locations each time. Excess M9 was removed with Kim-wipes. *C. elegans* reset their temperature preference if their cultivation temperature changes in less than 3 hr [15], so worm handling before the assay needs to be quick. Glycerol is poured on the assay plate and the dish is placed on top, leaving no air bubbles between the petri and the aluminum of the gradient plate. The two feedback-loop thermometers are placed in position L (p12) and R (p11) of the lid. The third can be placed in positions 1 to 10 (optional). The assay duration can vary from 35 minutes to 60 minutes.

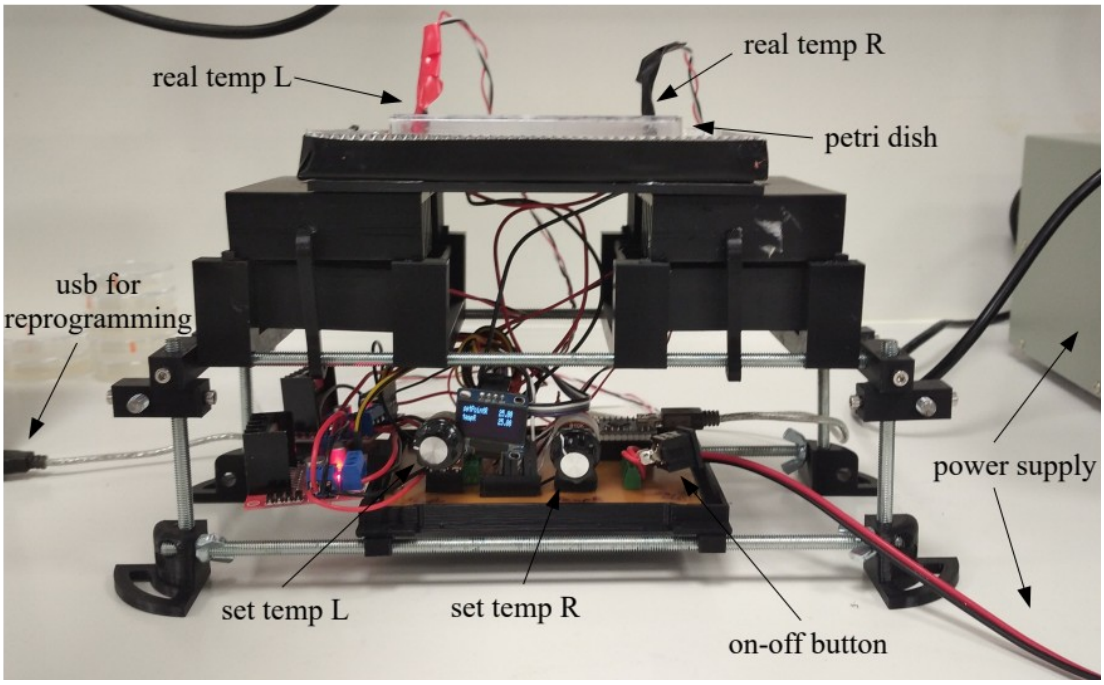

Figure 21. Photograph of the setup during testing

After the assay:

At the predetermined time for the completion of the assay, the dish is removed from the device and the worms are immobilized by the addition of a few drops of chloroform on the inside of the plate's original lid. The dish is inspected in a Leica MZ 8 stereo microscope. For counting, each worm is assigned a box number representing its location (see Figure 18). The percentage of worms on each isothermal is calculated. The starting boxes are excluded from the calculations to avoid worms that did not navigate from their initial placement due to injury.

C.2. Thermotaxis Assays – Results

For the worm thermal gradient assays, we used temperature ranges that include room temperature (~ 22 ^{o}C) and cultivation temperature i.e., from 20 to 23 ^{o}C, and gradient steepness between 1.5 and 0.5

ºC. Initial placements of the worms on the dish differed regarding the T_c x(cm) distance, to urge longer or shorter worm walks.

We find that day 1 worms migrate towards T_c, regardless the migration distance, with high gradient steepness negatively affecting the specificity (width) but not the peak position of the distribution. This can be seen in the comparison of Figure 22 to Figure 23. Mixed populations at high steepness show very low distribution specificity, even after 90 min, as shown in Figure 25. Figure 26 shows an assay with worms that remained in M9 for 1 hour before the assay. These worms remained in the location of their initial placement and did not migrate for the first 35 minutes of the assay. This observation indicates that stressful conditions can affect the worm performance in the thermal gradient assay. Over-wiping before the assay may also cause stress or impair locomotion even in not visibly harmed worms. This will change the outcome even at a 60' assay, as can be seen in Figure 24.

Figures 22-28 show representative assays with results of the discussed matters. The distribution of the population percentage at each isothermal is shown in each case.

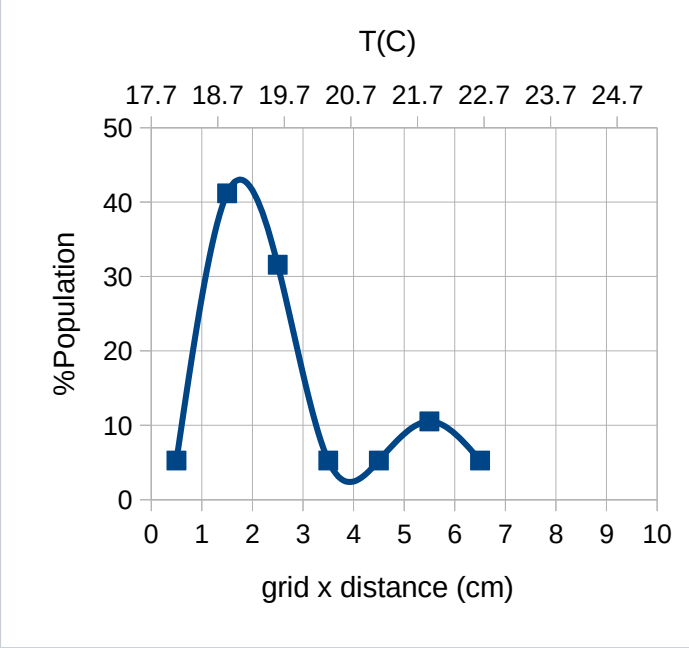

Figure 22. Assay 1: T_l = 18 ºC, T_h = 25 ºC, cultivation T_c = 20 ºC, assay duration 45 min. Day 1 worms were placed at the center of the dish and left undisturbed for 30 min before the start of the assay.

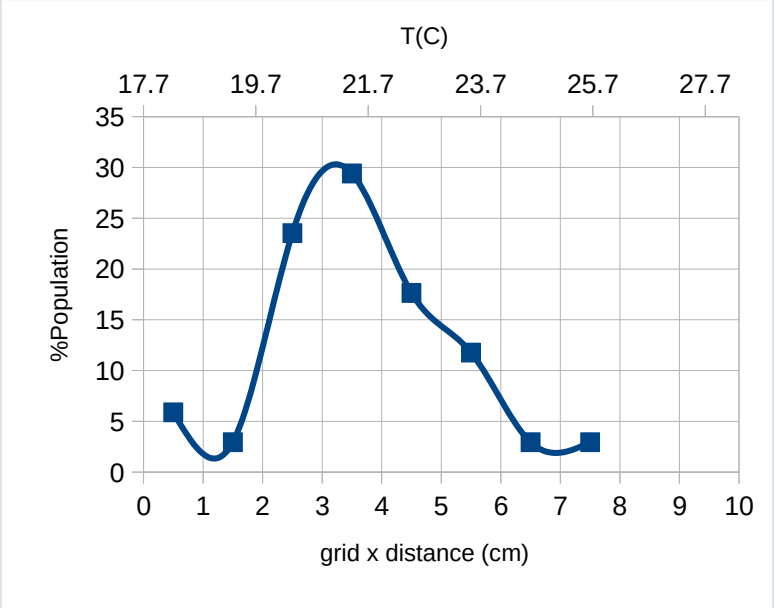

Figure 23. Assay 2: T_l = 18 ºC, T_h = 28 ºC, cultivation T_c = 20 ºC, duration 60 min. Day 1 worms were placed at both edges of the dish.

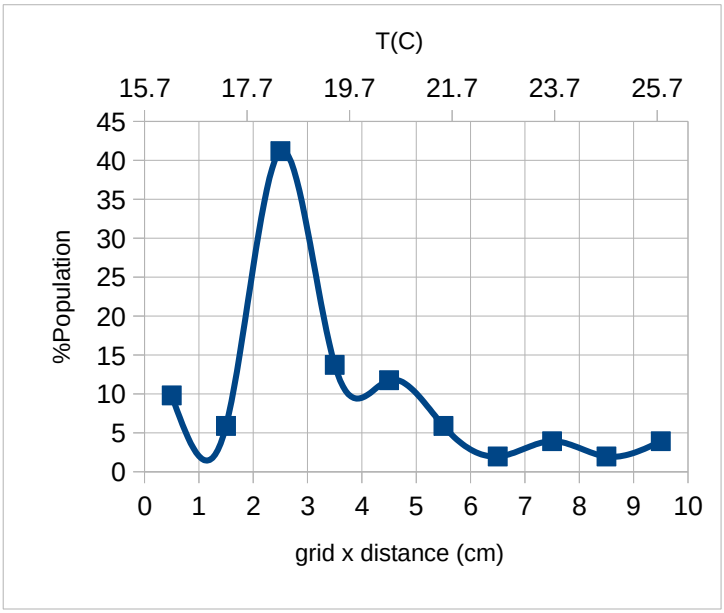

Figure 24. Assay 3: T_l = 16 ºC, T_h = 26 ºC, cultivation T_c = 20 ºC, duration 60 min. Day 2 worms were placed at the left edge of the dish. Over-wiping of M9 altered the resulting distribution.

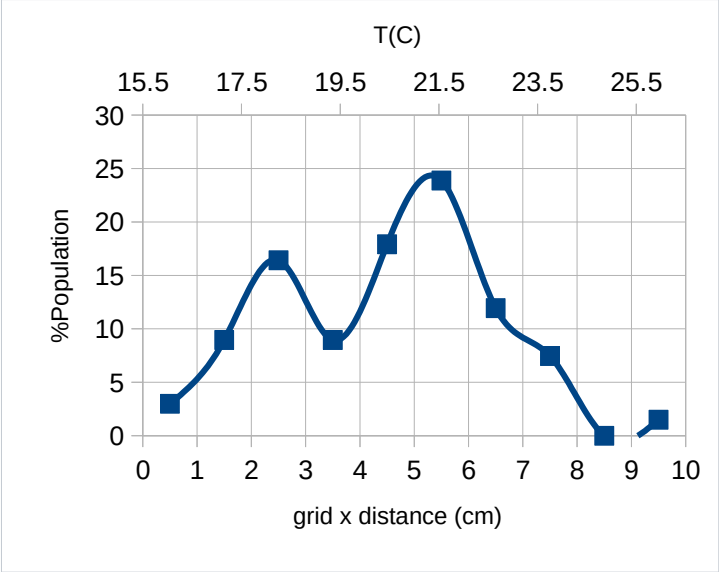

Figure 25. Assay 4: T_l = 16 ºC, T_h = 26 ºC, cultivation T_c = 20 ºC, duration 90 min. Mixed worm population (only adults counted) was placed at both edges of the dish.

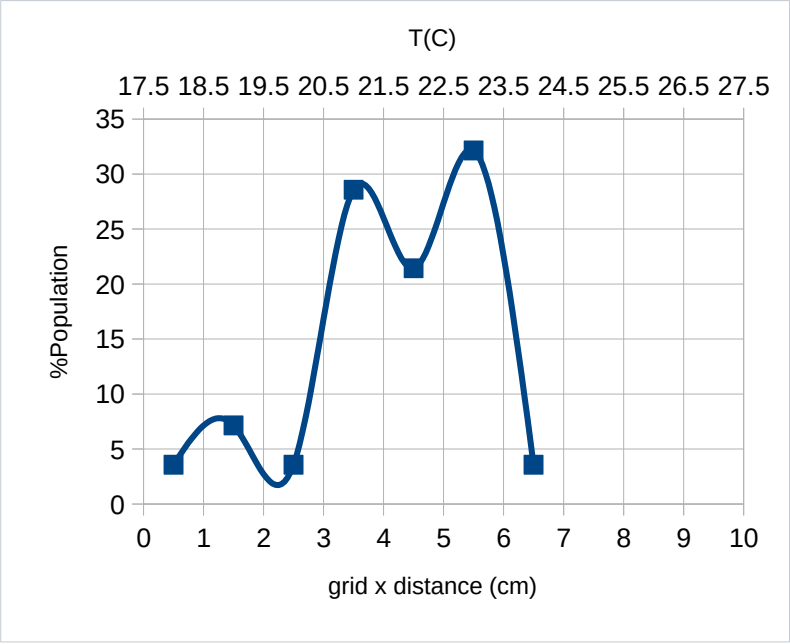

Figure 26. Assay 5: T_l = 18 ºC, T_h = 27 ºC, cultivation T_c = 20 ºC, duration 35 min. Day 2 worms were placed at the center of the dish, after 60 min in M9 at 23 ºC.

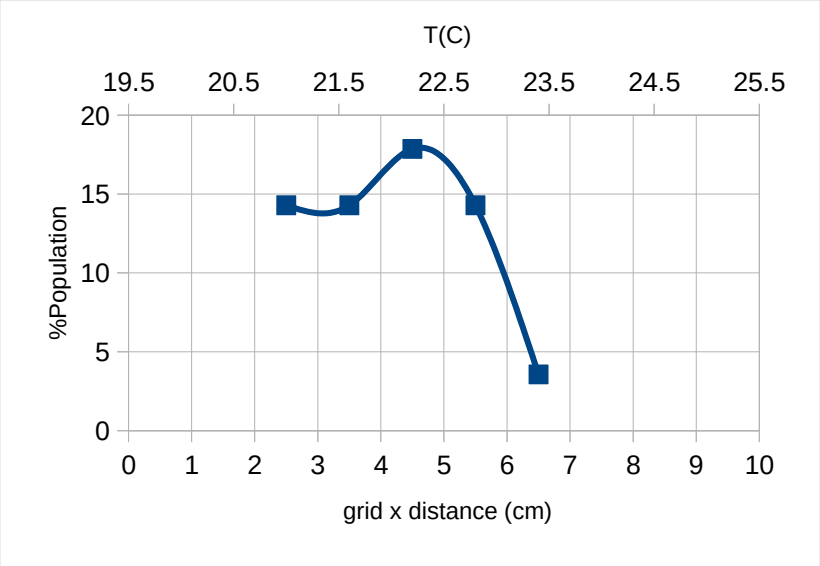

Figure 27. Assay 6: T_l = 20 ºC, T_h = 25 ºC, cultivation T_c = 21.5 ºC, duration 45 min. Day 1 worms were placed at the left edge of the dish.

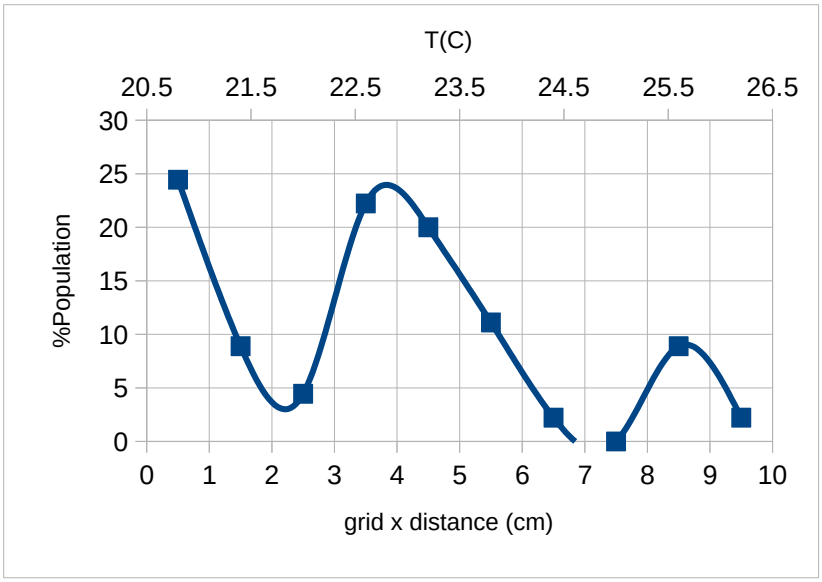

Figure 28. Assay 7: T_l = 20 ºC, T_h = 25 ºC, cultivation T_c = 21.ºC, duration 35 min. Day 1 worms were placed at the right edge of the dish.

D. Conclusions and Future steps

We showed that the TuReLi TTX assay plate is functional according to the operation standards of *C. elegans* thermotaxis studies.

Table 4: Prototype – Specifications

Time to steady state	≤ 7min	**Cost**	~80€
Deviation	±0.2 - ±0.4 ºC	**Dimensions**	(25×15×24)cm
R^2	0.985 – 0.999	**Weight**	400 gr
Power supply	12V/3A	**Test runtime**	90 min

We performed several assays testing thermal gradient settings, suggested by the literature [4][5][6] [11][12][13][14][16][17], and made similar observations. Thermal preferences of worms depend on cultivation conditions, feeding, worm age, population size during an assay, gradient steepness and more. Such parameters will determine the distribution shape, sharpness and peak location of the worm population on the dish under measurement. Well fed, young adults, grown under stable temperature will migrate towards that temperature, regardless the walk distance and direction, at $\Delta T \leq 0.9$ ºC/cm.

The system can be adjusted based on to commercially available parts and alternative options are presented below. In contrast to usual gradients on metal surfaces, gradients on NGM in plastic petri dishes that has low thermal conductivity, require faster response time. Thus, thermocouples can be used instead of Dallas thermometers (part 9, Table 2), with an appropriate modification of the Arduino sketch. As for the H-Bridge (part 5, Table 2), a more modern chip can be selected, a board that will be adequate for the two current-hungry peltiers, instead of the two in parallel wired here.

For the future, we intend to design a removable box cover to insulate the circuit board. A full device enclosure is not preferred as it would limit the accessibility to the moving/adjustable parts. Moreover, we are planning a TuReLi version with an added imaging system for real time monitoring. This module will report starting and final worm positions of the worms and track their routes (length and duration of movement). This will remove any user-biases, automate the quantification procedure and eliminate worm damage as worms won't be anesthetized at the end of the assay. The imaging system part will

consist of a RaspberryPi and camera, a frame assembled from 6 aluminum rods ⌀6 mm, 3D printed parts 8 (lower joints), 9 (upper joints), 6b (box base) that are already available (Table1) and a new 3D printed part base for the camera module.

Overall, our TuReLi TTX device provides, at a minimum cost, a viable solution for *C. elegans* research labs with no performance discounts. Moreover, the open access codes and modules allow for full performance tunability by the user with the potential of the device's implementation in more applications.

References

[1]Temperature gradient plate for MFFT test Toimittaja (industrial physics, LLC) https://fi.vwr.com/store/product/18828117/temperature-gradient-plate-for-mfft-test

[2] CPV Thermal Gradient Bar, TECA https://www.thermoelectric.com/cold-plates/laboratory-use/temperature-gradient-bar/

[3] GRD1 Temperature gradient plate, Grant Instruments (Cambridge) Ltd https://sitefiles.camlab.co.uk/tempgrad.pdf

[4]Raiders, S., Klein, M., & Singhvi, A. (2022). Multiplexing Thermotaxis Behavior Measurement in Caenorhabditis elegans. *BIO-PROTOCOL*, *12*(7). https://doi.org/10.21769/bioprotoc.4370

[5] Tsukada, Y., Yamao, M., Naoki, H., Shimowada, T., Ohnishi, N., Kuhara, A., Ishii, S., & Mori, I. (2016). Reconstruction of Spatial Thermal Gradient Encoded in Thermosensory Neuron AFD in *Caenorhabditis elegans*. *The Journal of Neuroscience*, *36*(9), 2571–2581. https://doi.org/10.1523/jneurosci.2837-15.2016

[6]Takeishi, A., Takagaki, N., & Kuhara, A. (2020). Temperature signaling underlying thermotaxis and cold tolerance in *Caenorhabditis elegans*. *Journal of Neurogenetics*, *34*(3–4), 351–362. https://doi.org/10.1080/01677063.2020.1734001

[7]Yoon, S., Piao, H., Jeon, T. J., & Kim, S. M. (2017). Microfluidic Platform for Analyzing the Thermotaxis of C. elegans in a Linear Temperature Gradient. *Analytical Sciences*, *33*(12), 1435-1439. https://doi.org/10.2116/analsci.33.1435

[8]Mori, I., & Ohshima, Y. (1995). Neural regulation of thermotaxis in Caenorhabditis elegans. *Nature*, *376*(6538), 344–348. https://doi.org/10.1038/376344a0

[9]Hedgecock EM, Russell RL., (1975) Normal and mutant thermotaxis in the nematode Caenorhabditis elegans. Proc Natl Acad Sci U S A.;72(10):4061-5. doi: 10.1073/pnas.72.10.4061.

[10]Quach, K. T., & Chalasani, S. H. (2022). Flexible reprogramming of Pristionchus pacificus motivation for attacking Caenorhabditis elegans in predator-prey competition. *Current Biology*, *32*(8), 1675-1688.e7. https://doi.org/10.1016/j.cub.2022.02.033

[11]Park, J. S., Oh, G., Kim, J., Park, E. Y., & Shin, J. H. (2019). Reversible Thermal Gradient Device to Control Biased Thermotactic Response of C. elegans. *Analytical Sciences*, *35*(12), 1367–1373. https://doi.org/10.2116/analsci.19p194

[12]Huang, T., Matsuyama, H. J., Tsukada, Y., Singhvi, A., Syu, R., Lu, Y., Shaham, S., Mori, I., & Pan, C. (2020). Age-dependent changes in response property and morphology of a thermosensory neuron and thermotaxis behavior in *Caenorhabditis elegans*. *Aging Cell*, *19*(5). https://doi.org/10.1111/acel.13146

[13]Luo, L., Cook, N., Venkatachalam, V., Martinez-Velazquez, L. A., Zhang, X., Calvo, A. C., Hawk, J., MacInnis, B. L., Frank, M., Ng, J. H. R., Klein, M., Gershow, M., Hammarlund, M., Goodman, M.B., Colón-Ramos, D. A., Zhang, Y., & Samuel, A. D. T. (2014). Bidirectional thermotaxis in *Caenorhabditis elegans* is mediated by distinct sensorimotor strategies driven by the AFD thermosensory neurons. *Proceedings of the National Academy of Sciences*, *111*(7), 2776–2781. https://doi.org/10.1073/pnas.1315205111

[14]Kimata, T., Sasakura, H., Ohnishi, N., Nishio, N., & Mori, I. (2012). Thermotaxis of C. elegans as a model for temperature perception, neural information processing and neural plasticity. *Worm*, *1*(1), 31–41. https://doi.org/10.4161/worm.19504

[15]Ito, H., Inada, H., & Mori, I. (2006). Quantitative analysis of thermotaxis in the nematode Caenorhabditis elegans. *Journal of Neuroscience Methods*, *154*(1–2), 45–52. https://doi.org/10.1016/j.jneumeth.2005.11.011

[16]Matsuyama, H. J., & Mori, I. (2020). Neural Coding of Thermal Preferences in the Nematode *Caenorhabditis elegans*. *Eneuro*, *7*(3), ENEURO.0414-19.2020. https://doi.org/10.1523/eneuro.0414-19.2020

[17]Ryu, W. S., & Samuel, A. D. T. (2002). Thermotaxis in *Caenorhabditis elegans* Analyzed by Measuring Responses to Defined Thermal Stimuli. *The Journal of Neuroscience*, *22*(13), 5727-5733. https://doi.org/10.1523/jneurosci.22-13-05727.2002

[18]Ritchie, M. W., Dawson, J. W., & MacMillan, H. A. (2021). A simple and dynamic thermal gradient device for measuring thermal performance in small ectotherms. *Current Research in Insect Science*, *1*, 100005. https://doi.org/10.1016/j.cris.2020.100005

[19]Sayeed, O., & Benzer, S. (1996). Behavioral genetics of thermosensation and hygrosensation in Drosophila. *Proceedings of the National Academy of Sciences*, *93*(12), 6079–6084. https://doi.org/10.1073/pnas.93.12.6079

[20]Zang, J., Chen, J., Chen, Z., Li, Y., Zhang, J., Song, T., & Sun, B. (2021). Printed flexible thermoelectric materials and devices. *Journal of Materials Chemistry A*, *9*(35), 19439–19464. https://doi.org/10.1039/d1ta03647e

[21]Building a Benchtop PID Controller Raymond Rogers Keithley Instruments, Tektronix, Inc. https://download.tek.com/document/BenchtopPIDController_WhPaper.pdf

[22]S Brenner, THE GENETICS OF *CAENORHABDITIS ELEGANS*, *Genetics*, Volume 77, Issue 1, 1 May 1974, Pages 71–94, https://doi.org/10.1093/genetics/77.1.71

[23] Grace Zhong, Laurel Kroo, Manu Prakash (2022). Thermotaxis in an apolar, non-neuronal animal. https://doi.org/10.1101/2022.08.19.504474

[24]Riddle, D. L., Blumenthal, T., Meyer, B. J., & Priess, J. R. (Eds.). (1997). *C. elegans II*. (2nd ed.). Cold Spring Harbor Laboratory Press.

[25]Gong, J., Yuan, Y., Ward, A., Kang, L., Zhang, B., Wu, Z., Peng, J., Feng, Z., Liu, J., & Xu, X. S. (2016). The C. elegans Taste Receptor Homolog LITE-1 Is a Photoreceptor. *Cell*, *167*(5), 1252-1263.e10. https://doi.org/10.1016/j.cell.2016.10.053

[26]Xu, C., Zhao, M. X., Poo, M. M., & Zhang, X. H. (2008). GABAB receptor activation mediates frequency-dependent plasticity of developing GABAergic synapses. *Nature Neuroscience*, *11*(12), 1410–1418. https://doi.org/10.1038/nn.2215

[27]Onukwufor, J. O., Farooqi, M. A., Vodičková, A., Koren, S. A., Baldzizhar, A., Berry, B. J., Beutner, G., Porter, G. A., Belousov, V., Grossfield, A., & Wojtovich, A. P. (2022). A reversible mitochondrial complex I thiol switch mediates hypoxic avoidance behavior in C. elegans. *Nature Communications*, *13*(1). https://doi.org/10.1038/s41467-022-30169-y

[28]Palikaras, K., Mari, M., Petanidou, B., Pasparaki, A., Filippidis, G., & Tavernarakis, N. (2017). Ectopic fat deposition contributes to age-associated pathology in Caenorhabditis elegans. *Journal of Lipid Research*, *58*(1), 72–80. https://doi.org/10.1194/jlr.m069385

Appendices

Appendix A: Code

```
#include <L298NX2.h> //H-Bridge
#include <AutoPID.h> //PID
#include <DallasTemperature.h> //Dallas
#include <OneWire.h>

#include <SPI.h> //screen
#include <Wire.h>
#include <Adafruit_GFX.h>
#include <Adafruit_SSD1306.h>

//H-Bridge inputs
const unsigned int IN1_A = 6;
const unsigned int IN2_A = 7;
const unsigned int EN_A = 3;
const unsigned int IN1_B = 8;
const unsigned int IN2_B = 9;
const unsigned int EN_B = 10;

L298NX2 motors(EN_A, IN1_A, IN2_A, EN_B, IN1_B, IN2_B);

#define WIRE Wire

#define POT_PIN_L A2
#define OUTPUT_PIN_L 3
#define TEMP_PROBE_PIN_L 2
#define TEMP_PROBE_PIN_R 5
#define TEMP_PROBE_PIN_M 4
#define TEMP_READ_DELAY 10
#define OUTPUT_MIN_L 20
#define OUTPUT_MAX_L 255
#define POT_PIN_R A3
#define OUTPUT_PIN_R 10
#define OUTPUT_MIN_R 20
#define OUTPUT_MAX_R 255

#define KPLl 50
#define KILl 1
#define KDLl 65
#define KPLh 23
#define KILh 0.1
#define KDLh 82

#define KPRl 39
#define KIRl 1
#define KDRl 53
```

```
#define KPRh 35
#define KIRh 0.1
#define KDRh 82

double temperatureL, setPointL, outputL;
double tempL, setL, outputValLl;
double outputValLh;
double temperatureR, setPointR, outputR;
double tempR, setR, outputValRl;
double outputValRh;
double tempC;

Adafruit_SSD1306 display = Adafruit_SSD1306(128, 32, &WIRE);

OneWire oneWire[] = {TEMP_PROBE_PIN_L, TEMP_PROBE_PIN_R, TEMP_PROBE_PIN_M};
const int oneWireCount = sizeof(oneWire) / sizeof(OneWire);
DallasTemperature sensor[oneWireCount];

AutoPID myPIDLl(&tempL, &setL, &outputValLl, OUTPUT_MIN_L, OUTPUT_MAX_L, KPLl, KILl, KDLl);
AutoPID myPIDLh(&tempL, &setL, &outputValLh, OUTPUT_MIN_L, OUTPUT_MAX_L, KPLh, KILh, KDLh);
AutoPID myPIDRl(&tempR, &setR, &outputValRl, OUTPUT_MIN_R, OUTPUT_MAX_R, KPRl, KIRl, KDRl);
AutoPID myPIDRh(&tempR, &setR, &outputValRh, OUTPUT_MIN_R, OUTPUT_MAX_R, KPRh, KIRh, KDRh);


#define BUTTON_A PA15
#define BUTTON_B PC7
#define BUTTON_C PC5
#define WIRE Wire

unsigned long lastTempUpdate;
bool updateTemperatures() {
  if ((millis() - lastTempUpdate) > TEMP_READ_DELAY) {

    temperatureL = sensor[0].getTempCByIndex(0);
    temperatureR = sensor[1].getTempCByIndex(0);
    tempC = sensor[2].getTempCByIndex(0);

    lastTempUpdate = millis();

    for (int i = 0; i < oneWireCount; i++) {
      sensor[i].requestTemperatures();
    }
    return true;
  }
  return false;
}

unsigned long lastScreenUpdate;

void updateScreen() {

  if ((millis() - lastScreenUpdate) <= 5000)
  {
    display.clearDisplay();
    display.setCursor(0, 0);
    display.print("tempC");
    display.setCursor(80, 0);
```

```
    display.print(tempC);

    display.display(); // actually display all of the above
  }

  else if (5000 < (millis() - lastScreenUpdate) && (millis() - lastScreenUpdate) <= 7000) {
    display.clearDisplay();
    display.setCursor(0, 0);
    display.print("setPointL");
    display.setCursor(80, 0);
    display.print(setPointL);
    display.setCursor(0, 10);
    display.print("tempL");
    display.setCursor(80, 10);
    display.print(temperatureL);
    display.display();
  }

  else if (7000 < (millis() - lastScreenUpdate) && (millis() - lastScreenUpdate) <= 9000) {
    display.clearDisplay();
    display.setCursor(0, 0);
    display.print("setPointR");
    display.setCursor(80, 0);
    display.print(setPointR);
    display.setCursor(0, 10);
    display.print("tempR");
    display.setCursor(80, 10);
    display.print(temperatureR);
    display.display();
  }

  else {
    display.clearDisplay();
    lastScreenUpdate = millis();
  }
}

void setup() {
  Serial.begin(9600);
  pinMode(POT_PIN_L, INPUT);
  pinMode(POT_PIN_R, INPUT);
  pinMode(OUTPUT_PIN_L, OUTPUT);
  pinMode(OUTPUT_PIN_R, OUTPUT);

  DeviceAddress deviceAddress;
  for (int i = 0; i < oneWireCount; i++) {
    ;
    sensor[i].setOneWire(&oneWire[i]);
    sensor[i].begin();
    if (sensor[i].getAddress(deviceAddress, 0)) sensor[i].setResolution(deviceAddress, 12);
  }

  for (int i = 0; i < oneWireCount; i++) {
    sensor[i].requestTemperatures();
  }

  myPIDLl.setBangBang(4);
```

```
  myPIDLl.setTimeStep(10);
  myPIDRl.setBangBang(4);
  myPIDRl.setTimeStep(10);
  myPIDLh.setBangBang(4);
  myPIDLh.setTimeStep(10);
  myPIDRh.setBangBang(4);
  myPIDRh.setTimeStep(10);

  Serial.println("OLED FeatherWing test");
  display.begin(SSD1306_SWITCHCAPVCC, 0x3C); // Address 0x3C for 128x32
  Serial.println("OLED begun");
  display.display();
  delay(100);
  display.clearDisplay();
  display.display();
}

void loop() {
  updateTemperatures();
  int potL = analogRead(POT_PIN_L);
  setPointL = map (potL, 0, 1023, 5, 45);

  int potR = analogRead(POT_PIN_R);
  setPointR = map (potR, 0, 1023, 5, 45);

  if (setPointL <= (temperatureL + 0.1 )) {
    tempL = ( - temperatureL);
    setL = ( - setPointL);
    myPIDLl.run();
    motors.setSpeedA(outputValLl);
    motors.backwardA();
  }

  else {
    tempL = temperatureL;
    setL = setPointL;
    myPIDLh.run();
    motors.setSpeedA(outputValLh);
    motors.forwardA();
  }

  if (setPointR < (temperatureR - 0.1 )) {
    tempR = ( - temperatureR);
    setR = ( - setPointR);
    myPIDRl.run();
    motors.setSpeedB(outputValRl);
    motors.backwardB();
  }

  else {
    tempR = temperatureR;
    setR = setPointR;
    myPIDRh.run();
    motors.setSpeedB(outputValRh);
    motors.forwardB();
  }
```

```
  Serial.print(setPointL);
  Serial.print("\t");
  Serial.print(temperatureL);
  Serial.print("\t");
  Serial.print(setPointR);
  Serial.print("\t");
  Serial.print(temperatureR);
  Serial.print("\t");
  Serial.println(tempC);

  display.setTextSize(1.8);
  display.setTextColor(SSD1306_WHITE);
  updateScreen();
}
```

Appendix B: Dimension Models

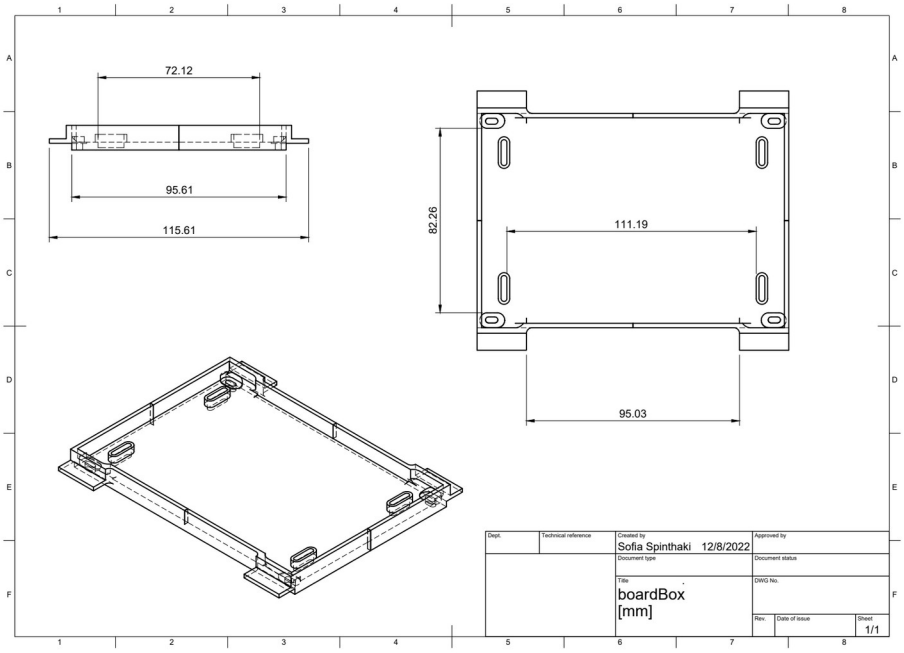

Figure 29. PCB base [mm], part 6a/Table 1

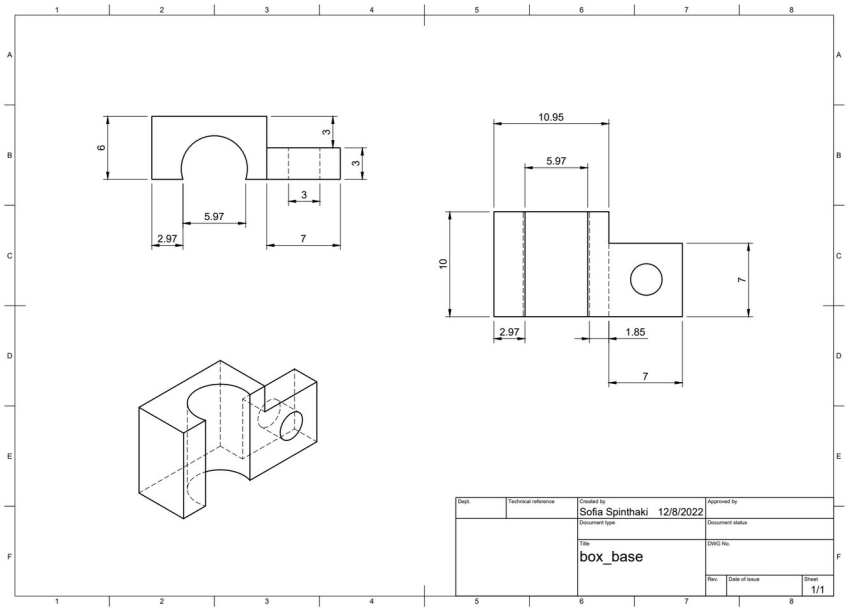

Figure 30. Box base [mm], part 6b/Table 1

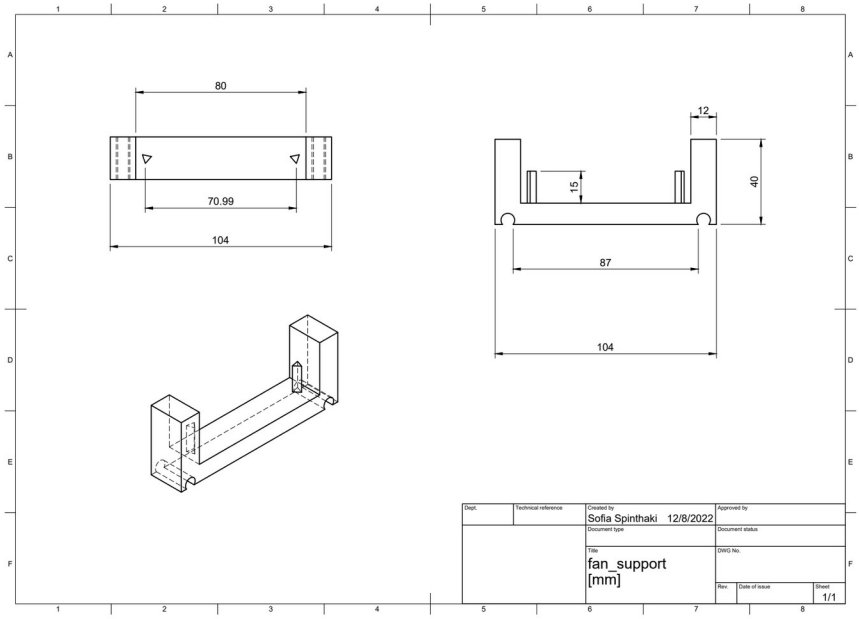

Figure 31. Fan support [mm], part 7/Table 1

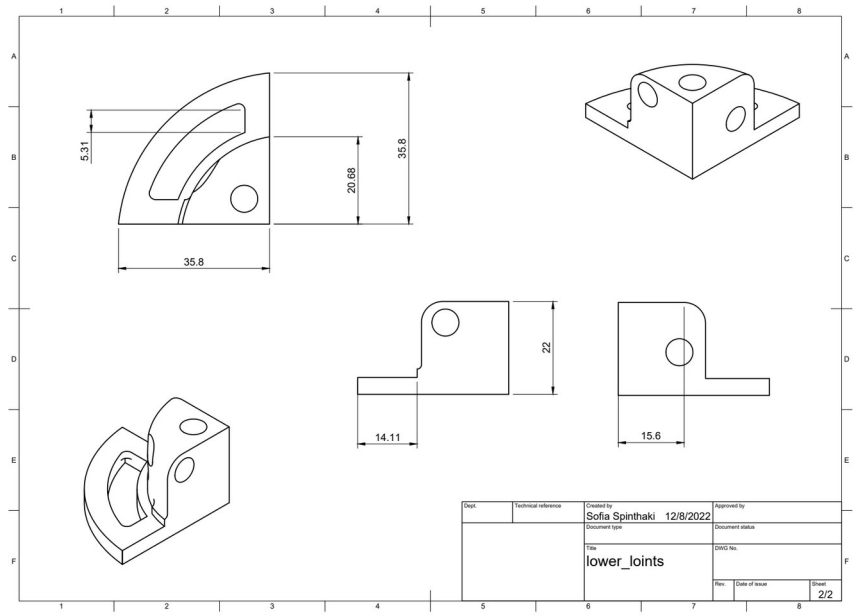

Figure 32. Lower joint [mm], part 8/Table 1

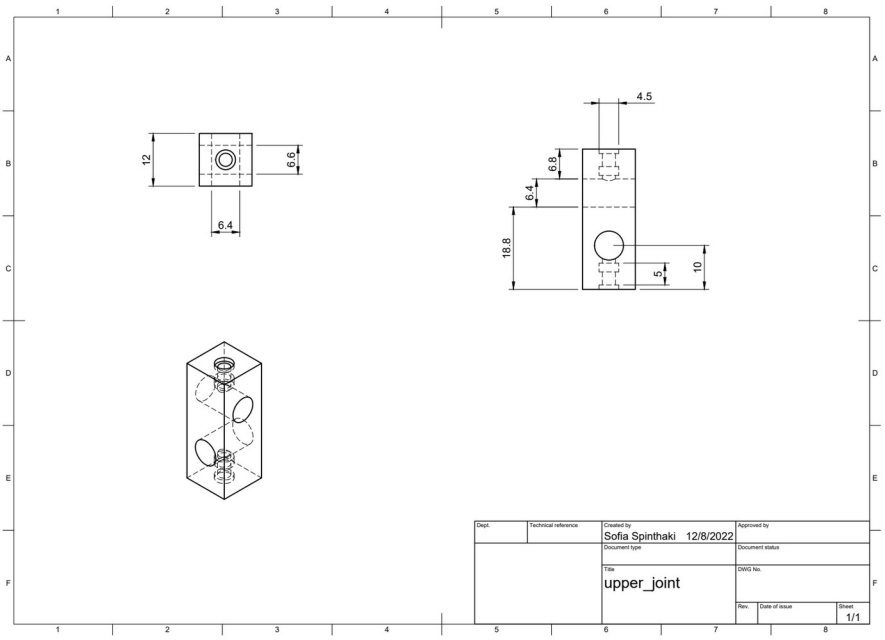

Figure 33. Upper joint [mm], part 9/Table 1

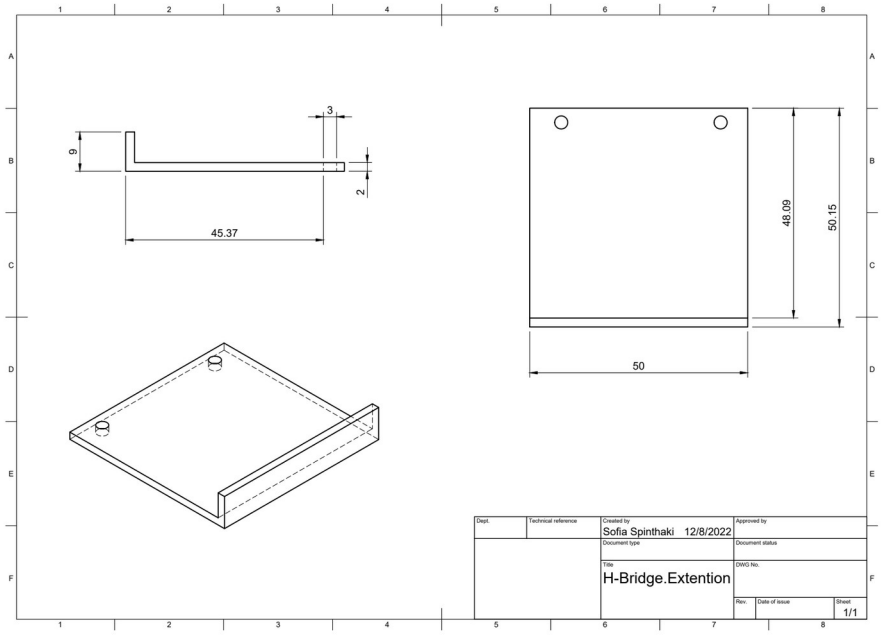

Figure 34. H-bridge extension [mm], part 10/Table 1

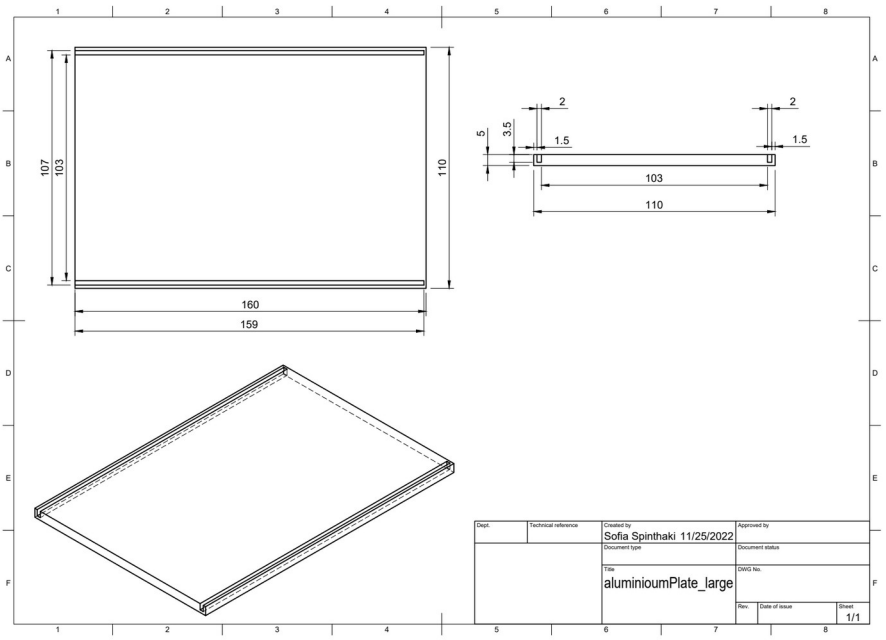

Figure 35. Aluminum plate large [mm], part 1/ Table 3

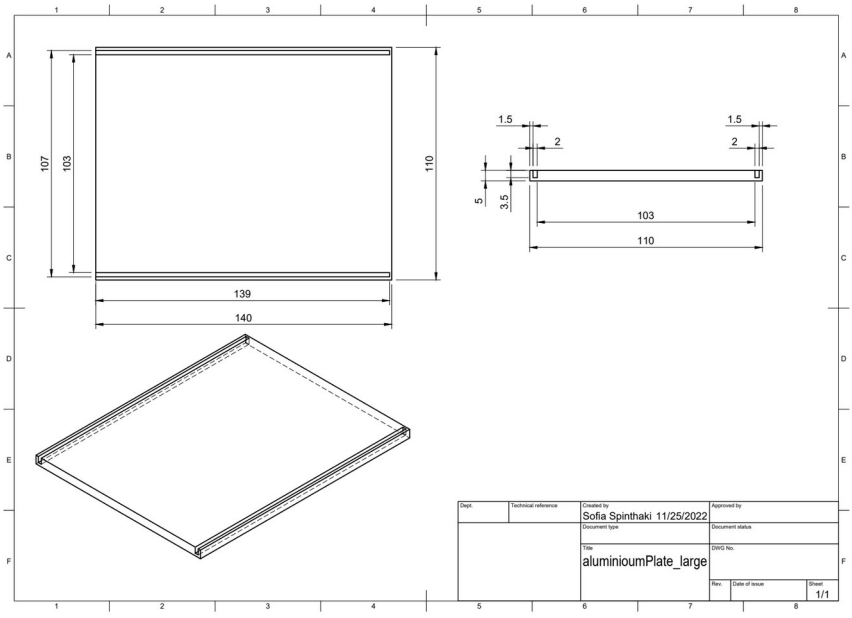

Figure 36. Aluminum plate medium [mm], part 1/ Table 3

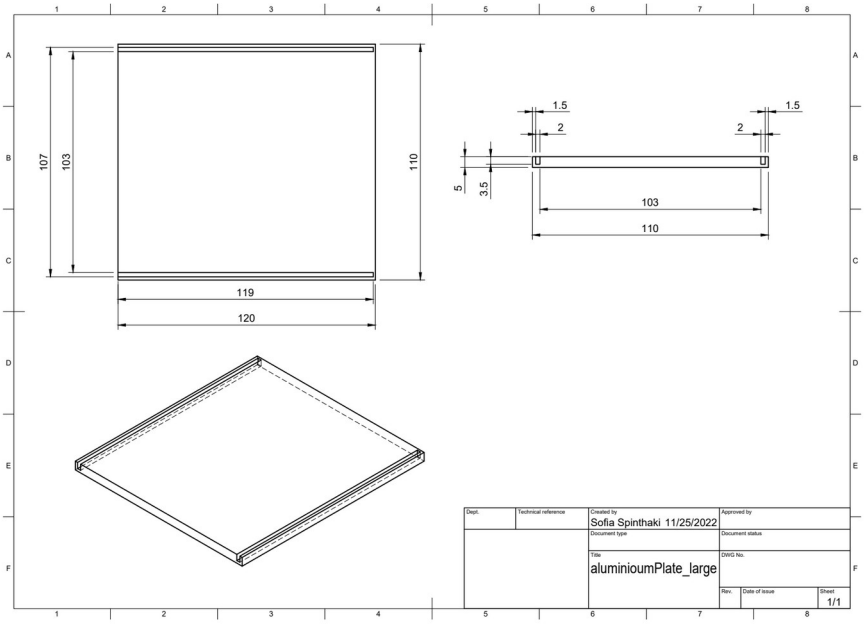

Figure 37. Aluminum plate small [mm], part 1/ Table 3

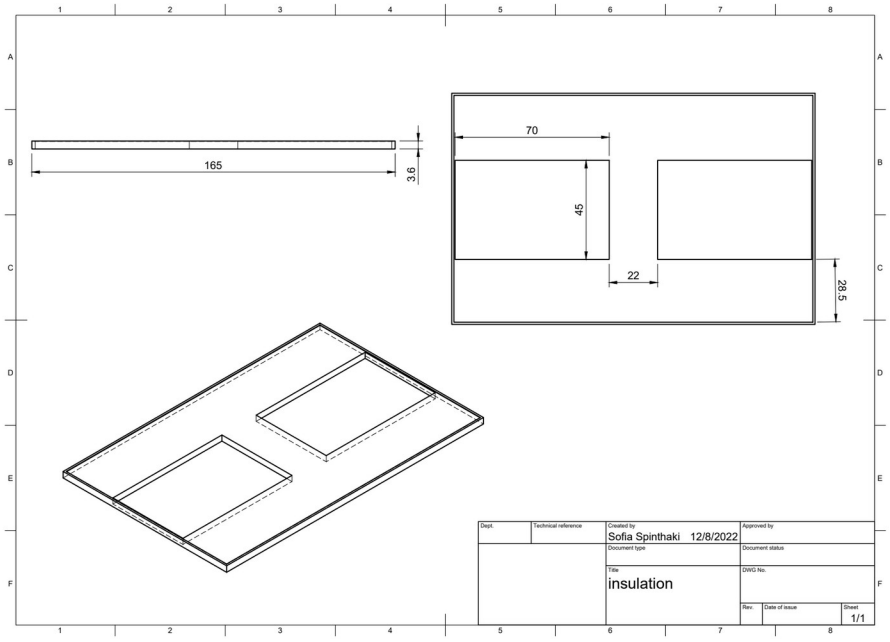

Figure 38. Insulating plate [mm], part 2/Table 3